AN ABSTRACT OF THE THESIS OF

Charles William Barrett for the degree of Master of Science in Geography presented on May 22, 1998. Title: Airborne Videography as a Classification and Validation Technique for Landsat TM-Based Vegetation Mapping.

Abstract approved:__

A. Jon Kimerling

The Oregon Department of Fish and Wildlife's (ODFW) Ecological Analysis Center (EAC) is in the process of creating, from Landsat Thematic Mapper (TM) imagery, a vegetation map of Oregon that will meet the latest standards set by the National Gap Analysis Program. Since field verification is often expensive and by nature intensive, ODFW wanted to determine the feasibility of using airborne videography to help classify and validate their Oregon vegetation map. In 1993, ODFW sampled approximately 4% of Oregon with airborne videography by flying north-south transects at 30-km intervals to be used for these purposes.

This research was designed to examine how and to what extent airborne videography can be used for assessing the accuracy of classified satellite imagery in vegetation mapping. An accuracy assessment strategy incorporating the ODFW airborne videography was developed and tested on a pilot study area consisting of the Luckiamute and Rickreall watersheds in western Oregon.

Airborne videography was found to have more potential as a classification aid than as an accuracy assessment tool. Its limited usefulness in accuracy assessment results primarily from the necessity to field verify any interpretation made of the videography

before it can be successfully incorporated into an accuracy assessment methodology. Additionally, the difficulty of obtaining a sufficient sample for all vegetation classes and the relatively poor spatial and spectral resolution of current airborne video systems impede its use in accuracy assessment. A field verification process combining global positioning system (GPS) and geographic information system (GIS) technologies with a laptop computer is outlined as a more efficient and accurate alternative to using the ODFW airborne videography for accuracy assessment of the Oregon vegetation map.

Master of Science thesis of Charles William Barrett presented on May 22, 1998

APPROVED:

Major Professor, representing Geography

Chair of Department of Geosciences

Dean of Graduate School

I understand that my thesis will become part of the permanent collection of Oregon State University libraries. My signature below authorizes release of my thesis to any reader upon request.

Charles William Barrett, Author

Airborne Videography as a Classification and Validation Technique for Landsat TM-Based Vegetation Mapping

by

Charles William Barrett

A THESIS

submitted to

Oregon State University

in partial fulfillment of
the requirements for the
degree of

Master of Science

Presented May 22, 1998
Commencement June 1999

ACKNOWLEDGMENT

I would like to take this opportunity to thank all those who made this work possible.

First, I would like to thank the Oregon Department of Fish and Wildlife's Ecological Analysis Center and the Environmental Protection Agency for funding my research. Additionally, I would like to thank and acknowledge all the members of the Ecological Analysis Center for their support and guidance throughout this research. A special thanks goes to Chris Kiilsgaard and Clair Klock for giving me so much of their time and for sharing their vast knowledge of Oregon's vegetation.

I would like to acknowledge and thank my Committee members, Dr. A. Jon Kimerling, Dr. Charles Rosenfeld, Dennis White and Dr. John Bolte for their guidance and editorial help. Thanks also to the faculty and staff of the Oregon State University Geography Program for their support.

I owe a special thank you to Patricia Berger for all of her support and encouragement throughout this research endeavor. Thank you so much Pat!

Finally, thank you Evan Hoy, World's Greatest Hound, for all those mind-clearing walks and pleasant distractions from this research.

TABLE OF CONTENTS

TABLE OF CONTENTS (Continued)

Page

LIST OF FIGURES

LIST OF TABLES

AIRBORNE VIDEOGRAPHY AS A CLASSIFICATION AND VALIDATION TECHNIQUE FOR LANDSAT TM-BASED VEGETATION MAPPING

1. INTRODUCTION

1.1 Problem Definition

The Oregon Department of Fish and Wildlife's (ODFW) Ecological Analysis Center (EAC) is in the process of creating, from Landsat Thematic Mapper (TM) satellite imagery, a vegetation map of Oregon that will meet the latest standards set by the U. S. Geological Survey, Biological Resources Division (GAP). At least 32 other states are producing, or have produced, similar maps with Landsat TM data (Scott et al. 1993; M. Jennings, University of Idaho, personal comm.). Typically, identification and labeling of vegetation polygons has involved on-screen interpretation along with supervised and unsupervised classification aided by ancillary vegetation data. However, limited field verification of these Landsat TM-based maps has been conducted since field verification is often expensive and by nature intensive. Some states such as Arizona, Texas, and the New England Regional Program have attempted using low-altitude aerial videography to supplement ground observations for labeling and accuracy assessment of satellite imagery (Graham 1993; J. Finn, University of Massachusetts, personal comm.; T. McKinney, Texas Tech University, personal comm.). In a similar manner, ODFW desires to use airborne videography acquired in 1993 for developing and assessing the accuracy of its vegetation map of Oregon.

As mentioned above, investigation into the use of airborne videography for the classification and validation of satellite imagery is already underway. The Vermont Cooperative Fish and Wildlife Unit has gone so far as to develop an air-video interpretation station that integrates video, satellite imagery, and GIS data for land-cover mapping in Vermont as part of the GAP (Schlagel, 1995). Schlagel's work with this air-

video interpretation station has focused on using airborne videography in training site selection. Besides these few examples, however, little has been written on the use of airborne videography for classification and accuracy assessment of satellite imagery.

This research was designed to further examine how airborne videography can be used for the classification of satellite imagery and for assessing the accuracy of classified satellite imagery in vegetation mapping. More specifically, an accuracy assessment strategy incorporating airborne videography was developed and tested on a pilot study area consisting of the Luckiamute River and Rickreall Creek watersheds in the Willamette Valley of western Oregon. The results of this research will be used by ODFW when developing an accuracy assessment strategy for the remainder of its Landsat TM-based vegetation map of Oregon and for determining how it might efficiently collect and implement airborne videography in future mapping projects.

1.2 Statement of Purpose

The goal of this research is to determine how and to what extent airborne videography can replace field checking in the classification and/or accuracy assessment of satellite-based vegetation maps. Four objectives address this goal. The two primary objectives are:

1) To use videography to determine the classification accuracy of the vegetation map created for the pilot study area;
2) To assess the utility of airborne videography as a classification and validation technique for the Landsat TM-based vegetation map of Oregon.

Additional objectives included:

3) To estimate the best scale of aerial videography acquisition for use in Landsat TM vegetation mapping accuracy assessments;
4) To develop a suitable methodology for using airborne videography in accuracy assessments of future Landsat TM-based vegetation maps.

Objective 1 was accomplished by georectifying sample transects of airborne videography, visually interpreting these images, field-verifying them, and statistically comparing the resulting classification to the ODFW Landsat TM-based vegetation map produced for the study area. The visually-interpreted video was also statistically compared to the field-interpreted video. A critical evaluation of these results achieved Objective 2. Comparing videography acquired at three different scales addressed Objective 3. Objective 4 was completed based on the successes and problems encountered in the accuracy assessment methodology tested in the pilot study area and on information resulting from an extensive literature review.

The following chapters will: 1) review the existing literature pertaining to accuracy assessment techniques for maps produced from remotely sensed data, and advancements in airborne videography technology; 2) describe the study area, and discuss the methodology developed for assessing the use of airborne videography as an accuracy assessment tool; 3) discuss the results of the pilot study area accuracy assessment; and 4) make recommendations for using airborne videography in the accuracy assessment of the ODFW Landsat TM vegetation map of Oregon and in future mapping projects based on the findings of this research.

2. LITERATURE REVIEW

An understanding of accuracy assessment techniques for vegetation mapping and of airborne videography was needed before methodologies could be determined in this study. A literature search was conducted in two major areas: 1) accuracy assessment techniques for maps produced from remotely sensed data; and 2) advancements in airborne videography technology.

2.1 Accuracy Assessment Techniques for Remotely Sensed Maps

The development of accuracy assessment techniques for land cover mapping from remotely sensed data has been recently presented in detail by Russell G. Congalton (1996). Therefore, the contents of this section are based on Congalton's findings except where otherwise noted.

Congalton suggests that the history of accuracy assessment of digital remotely sensed data can be divided into four epochs beginning around 1975. Prior to 1975, "field checking was performed as part of the interpretation process, but no overall map accuracy or other quantitative measure of quality was routinely produced (Congalton, 1996)." An "it looks good" mentality prevailed during the first epoch which was characterized by no rigorous accuracy assessment being performed. The second epoch is termed the "epoch of non-site specific assessment" because overall area totals for each class were compared between ground estimates and the map without regard for location. The "epoch of site specific assessment" followed this short-lived stage. A site specific assessment compares actual ground locations to the corresponding area on the map to produce a measure of overall accuracy. The fourth and current epoch can be termed the "age of the error matrix." This epoch includes an evolving number of analysis techniques based on the development of an error matrix. "An error matrix is a square

array of numbers set out in rows and columns which expresses the number of sample units (i.e., pixels, clusters of pixels, or polygons) assigned to a particular category relative to the actual category as verified by some reference data (Congalton and Green, 1993)."

An assumption underlying the error matrix technique is that all differences between the remotely sensed classification and the reference data are due to classification and/or delineation error. There are, however, other potential sources of confusion between the remotely sensed classification and the reference data that must be considered. Possible sources of error include:

1) Registration differences between the reference data and the remotely sensed map classification;
2) Delineation error encountered when the sites chosen for accuracy assessment are digitized;
3) Data entry error when the reference data are entered into the accuracy assessment database;
4) Error in interpretation and delineation of the reference data (e.g., photointerpretation error);
5) Changes in land cover between the date of the remotely sensed data and the date of the reference data (temporal error), for example, changes due to fires, urban development or harvesting;
6) Variations in classification and delineation of the reference data due to inconsistencies in human interpretation of heterogeneous vegetation;
7) Errors in the remotely sensed map classification; and
8) Errors in the remotely sensed map delineation (Congalton and Green, 1993).

The first six factors are non-error classification differences that can significantly lower the accuracy in an error matrix and make the classification (i.e., factors 7 and 8) look worse than it actually is. Methods must be designed and incorporated to control for the first six factors when using an error matrix approach to accuracy assessment (Congalton and Green, 1993).

An error matrix is an effective way to represent accuracy because it allows overall accuracy and the accuracy of each class to be determined, as well as errors of inclusion (commission errors) and exclusion (omission errors) present in the classification. Overall

accuracy is calculated by dividing the total correctly classified sample units by the total number of sample units in the matrix. The accuracy of each class can be calculated similarly; however, the total number of correctly classified sample units in a class may be divided by either the total number of sample units for that class in the classified map or the total number of sample units for that class in the reference data. The former is a measure of commission error termed "users accuracy" and represents the probability that a sample unit classified on the map actually represents that class on the ground. The latter, termed "producers accuracy," measures omission error or the probability of a reference sample unit being correctly classified (Story and Congalton, 1986).

Congalton states that the error matrix is also an appropriate basis for many analytical statistical techniques, especially discrete multivariate techniques. Beginning in 1983, discrete multivariate techniques have been used for accuracy assessment of remotely sensed data classifications by many researchers (e.g., Congalton et al., 1983; Rosenfield and Fitzpatrick-Lins, 1986; Hudson and Ramm, 1987; Campbell, 1987; Lillesand and Kiefer, 1994). "Discrete multivariate techniques are appropriate because remotely sensed data are discrete rather than continuous. The data are also binomially or multinomially distributed rather than normally distributed. Therefore, many common normal theory statistical techniques do not apply (Congalton, 1996)."

Two popular . discrete mutivariate analytical techniques used in accuracy assessment, after an error matrix is developed, are "MARGFIT" (Congalton et al., 1983) and "KAPPA" (Cohen, 1960). MARGFIT normalizes the matrix using an "iterative proportional fitting procedure which forces each row and column in the matrix to sum to one. ... In this way, differences in sample sizes used to generate the matrices are eliminated and therefore, individual cell values within the matrix are directly comparable. Also, because the iterative process totals the rows and columns, the resulting normalized matrix is more indicative of the off-diagonal cell values (i.e., the errors of omission and commission) than the original matrix (Congalton et al., 1983)."

KAPPA analysis yields a KHAT statistic (an estimate of KAPPA) which is another measure of agreement. The formula for computing the KHAT statistic can be found in Bishop et al. (1975) and Congalton (1996). The benefit of KAPPA analysis is that it provides two statistical tests of significance. First, the map classified from remotely sensed data can be tested to see if it is significantly better than a map generated by randomly assigning labels to areas. Second, any two matrices can be compared to determine if they are significantly different statistically.

Despite the popularity of KAPPA analysis for accuracy assessment of image classification, Ma and Redmond (1995) argue that the Tau coefficient is a better tool. Like KAPPA, the Tau coefficient also measures the improvement of a classification over a random assignment of pixels to groups. However, the Tau coefficient better adjusts percentage agreement than Kappa, and it is easier to calculate and interpret.

None of these techniques address the recently developing concern that many classification systems promote subjectivity when distinguishing supposed mutually exclusive classes. Complex classification schemes, for example, may yield increased variation in human interpretation which can have a significant impact on what is considered correct and incorrect. In other words, the line between mutually exclusive classes becomes fuzzier as the number of classes increases, and the chances of a sample unit being classified the same by different researchers decreases. Using an error matrix in these cases would help identify sources of confusion but would likely result in an incorrect assessment of error.

New analytical techniques, some of which build on the error matrix, are being developed to address these complexities. For example, the substitution of fuzzy set theory for classical set theory has been suggested (Woodcock, 1996; Milliken and Woodcock, 1996). Congalton cites Gopal and Woodcock's (1994) proposal to use fuzzy sets to "allow for explicit recognition of the possibility that ambiguity might exist regarding the appropriate map label for some locations on the map." A fuzzy sets

approach would recognize "that instead of a simple system of correct (agreement) and incorrect (disagreement) there can be a variety of responses such as: absolutely right, good answer, acceptable, understandable but wrong, and absolutely wrong (Congalton, 1996 from Gopal and Woodcock, 1994)." A fuzzy sets approach provides significantly more information and a better understanding of the classification error to the analyst than does the traditional error matrix. However, it is much more complex to implement than the traditional error matrix, and it does not result in a simple number (i.e., percentage of accuracy) that many map users desire.

Choosing the appropriate sample size for assessing the accuracy of remotely sensed data has been another major concern of researchers (Van Genderen and Lock, 1977; Tortura, 1978; Hay, 1979; Hord and Brooner, 1976; Rosenfield et al., 1982; Congalton, 1988b). Most researchers, however, have used an equation based on the binomial distribution or the normal approximation to the binomial distribution. Congalton explains that these techniques are not appropriate for determining the sample size when using an error matrix. Instead, an equation based on the multinomial distribution, as suggested by Tortura (1978), should be used.

Additionally, traditional thinking about sampling usually does not apply to remotely sensed data because of the large number of pixels in an image. "A balance between what is statistically sound and what is practically attainable must be found (Congalton, 1996)." Congalton has found that "a good rule of thumb seems to be collecting a minimum of 50 samples for each vegetation or land use category in the error matrix. This rule also tends to agree with the results of computing sample size using the multinomial distribution (Tortura, 1978)." If the area being sampled is larger than a million acres or the classification has more than 12 categories, the minimum number of samples should be increased to 75 to 100 samples per category. Also, it may be desirable to take more samples in categories of greater interest and reduce the number of samples in categories of less interest within the objectives of the mapping project. More samples

could also be taken in categories that show greater variability, such as uneven-aged forests, with less samples taken in categories, such as water, that have low variability.

Sampling scheme is also a critical component of accuracy assessment in that the samples contained in an error matrix must be representative of the study area. Many researchers have addressed the topic of sampling schemes for accuracy assessment of remotely sensed data (Rosenfield et al., 1982; Congalton, 1988b; Congalton, 1991; Stehman, 1992; Stehman, 1996), but opinions about proper sampling scheme vary greatly and "include everything from simple random sampling to stratified systematic unaligned sampling (e.g., Hord and Brooner, 1976; Rhode, 1978; Ginevan, 1979; Fitzpatrick-Lins, 1981)." Little research, however, has been done to specifically evaluate sampling schemes for accuracy assessment of remotely sensed data, and no clear consensus as to the best scheme has been established.

"Congalton (1988b) performed sampling simulations on three spatially diverse areas (forest, agriculture, and rangeland) and concluded that in all cases simple random without replacement and stratified random sampling provided satisfactory results." However, simple random sampling tends to under sample small but potentially important areas unless very large sample sizes are obtained. Therefore "stratified random sampling is recommended where a minimum number of samples are selected from each strata (i.e., category) (Congalton, 1996)."

Implementing any type of random sampling scheme may, however, be "somewhat impractical because of having to collect ground information for the accuracy assessment at random locations on the ground" which may be very difficult or impossible to access. Some type of systematic approach would make the collection of ground information easier. However, "results of Congalton (1988a) showed that periodicity in the errors as measured by autocorrelation analysis could make the use of systematic sampling risky for accuracy assessment." Therefore, Congalton suggests that some combination of random and systematic sampling may yield the best balance between

statistical validity and practical application. "Such a system may employ systematic sampling to collect some assessment data early in a project while random sampling within strata would be used after the classification is completed to assure enough samples were collected for each category and to minimize any periodicity in the data (Congalton, 1996)."

Two factors that may potentially affect the results of an accuracy assessment and which, therefore, must be elaborated are spatial autocorrelation, and edge and boundary effects. Spatial autocorrelation occurs "when the presence, absence or degree of a certain characteristic affects the presence, absence or degree of the same characteristic in neighboring units (Congalton, 1996 from Cliff and Ord, 1973)." If an error at a given location influences errors at nearby locations in a classification, this spatial autocorrelation becomes significant to the accuracy assessment (Campbell, 1981). Congalton (1988a) showed such a positive correlation, as much as 30 pixels (over 1 mile) away, when assessing classified Landsat MSS data of an agriculture, a range, and a forest site. Spatial autocorrelation, therefore, must be considered when selecting the sample scheme and sample size for accuracy assessment. Most importantly, autocorrelation may affect the assumption of sample independence in that it could cause periodicity in the data that could affect the results of any type of systematic sample.

Edge and boundary effects result from trying "to divide a rather continuous environment called Earth into a number of discrete categories (Congalton, 1996)." The problem is deciding where the boundary lines should be drawn between different cover types on the ground. As mentioned previously, this delineation becomes more difficult as the classification scheme increases in complexity. Traditional accuracy assessment techniques have tried to avoid the influence of boundary effects by taking samples near the centers of polygons or at least away from the edges. However, "with the use of global positioning systems (GPS) and the improvement in positional accuracy of individual

pixels, methods to assess boundary issues can be developed and incorporated into the assessment routines (Congalton, 1996 from Chrisman, 1989; Goodchild, 1989)."

2.2 Airborne Videography as a Remote Sensing Tool

Mausel et al. (1992) established that serious interest in airborne videography as a remote sensing tool has existed for approximately fifteen years (e.g., Manzer and Cooper, 1982; Edwards, 1982; Escobar et al., 1983; Vlcek, 1983; Everitt et al., 1991). During this time, airborne videography has been used by researchers for a variety of purposes as demonstrated by the following examples:

- Range management (Everitt and Nixon, 1985);
- Wetland classification (Jennings et al., 1992);
- Agricultural assessment (Everitt et al., 1991);
- Vegetation mapping (Graham, 1993; Thomasson et al., 1994);
- Environmental impact evaluation (Snider et al., 1994);
- Natural disaster impact assessment (Doyle et al., 1994); and
- Land cover / land use mapping (Limaye et al., 1994).

Recently, there has been an increasing interest in using airborne videography for collecting ground-truth data for satellite image interpretation and post-classification accuracy assessment (Graham, 1993; Schlagel, 1995; Slaymaker et al., 1996).

The features of airborne videography that have made it an attractive sensor for this variety of applications are its:

1) low cost;
2) real-time or near-real-time availability of imagery for visual assessment or computer image processing analysis;
3) immediate potential for digital processing on the signal;
4) ability to collect spectral data in very narrow bands (5 to 12 nm) in the visible to near infrared (NIR);
5) ability to collect spectral data in the mid-infrared (1.35 to 2.50 μm) water absorption regions; and

6) data redundancy in which images are acquired every 1/30 second producing multiple views of a target or scene (Mausel et al., 1992).

Additionally, "because CCD [charge coupled device] sensors have higher light sensitivity than most film, airborne videography can often be flown under low light or hazy conditions that would be considered adverse for photography (King, 1992)."

Another advantage of videography is that location data from a global positioning system (GPS) receiver can be recorded and matched to each video frame. Systems incorporating this technology record the GPS time on the audio track of the video in place of the SMPTE (Society for Motion Picture and Television Engineers) time code signals (Graham, 1993). Often, the GPS time is placed directly on the video images as well. A GPS data file, containing time and location, is recorded simultaneously so that the location of the center point of each frame can be determined later.

These airborne GPS-video acquisition systems, however, are not perfect. First, GPS typically updates on a one-second interval which results in the same location being recorded for 30 frames (Graham, 1993). Second, aircraft shifts due to turbulence or a low accuracy GPS can result in the recorded location being substantially different than the actual location of the video frame's center, especially for higher altitude flights (Bobbe et al., 1993). Assessments of these airborne GPS-video acquisition systems have found positional errors for non-differentially corrected GPS locations as high as 148 meters (Graham, 1993) and up to 70 meters for differentially corrected GPS data (Slaymaker et al., 1996). Wanless (1992) has developed an advanced system that incorporates a two-axis vertical gyroscope and a servo-control motor on the camera mount for real-time adjustment of aircraft roll and pitch. This Digital Video Geographic (DVG) survey system has yielded 2-3 meter positional accuracy. Additionally, Thorpe (1993) claims that 10 cm airborne GPS accuracy is possible using specialized procedures for elimination of systematic errors.

The major disadvantage of video is its relatively low resolution when compared to film (Mausel et al., 1992; Everitt et al., 1991). Standard color video recorders have an image resolution of 240 lines across the format field and Super-VHS (S-VHS) recorders have 400 line resolution whereas color 35-mm slide film has potentially more than 1500 line resolution (Mausel et al., 1992; Lusch, 1988). Additionally, further image resolution degradation may result from the interlace-effect. Standard $1/30^{th}$-second video frames are comprised of two interlaced $1/60^{th}$-second fields. Because each field is acquired over a slightly different ground area (due to the forward motion of the airplane), their lines may overlap or there may be gaps in the terrain coverage (King, 1992; Russ, 1995). Analysis may, therefore, have to be performed on a single field (at lower resolution) rather than on a full frame (Meisner, 1986).

Other disadvantages of video are that the automatic gain control on most video cameras hinders radiometric calibration (Everitt et al., 1991), and brightness values tend to increase towards the side of the image opposite to the sun illumination direction (King, 1991). These features make temporal studies and automated classification techniques difficult. Airborne videography, therefore, commonly has been analyzed to compare relative spectral differences between features without attention to the absolute radiance or reflected differences being imaged (Mausel et al., 1992). However, increasing research efforts addressing radiometric correction and other technical questions (e.g., sensor noise and optical effects) in videography have shown promise (Palmer et al., 1987; King, 1991, 1992; Ehlers et al., 1989; Edwards and Schumacher, 1989; Gerbermann et al., 1989; Richardson et al., 1992).

A wide variety of airborne video acquisition systems, consisting of either a single camera or multiple cameras, have been successfully implemented. Mausel et al. (1992) and Everitt et al. (1991) describe in great detail this variety of systems and their applications. Single color video camera systems typically have been used for basic visual interpretation of general land-cover features. Applications using multiple recording

systems have often implemented "digital image processing to analyze, quantify, and classify narrow-band multispectral images, in both original and transformed data formats (e.g., ratioing, principal components, and texture) (Mausel et al., 1992 from Everitt et al., 1988; King and Vlcek, 1990; Mausel et al., 1990; Yuan et al., 1991)."

The future of airborne videography, along with digital frame cameras, is very promising. "The poor resolving power of videography is gradually being improved with the development of sensors having more photosites per unit dimension, Super VHS (and other advanced recording), higher sampling frequency digitizers, and high-resolution digital frame cameras that are not subject to NTSC scanning constraints (King, 1992)." Airola (1996), for example, summarizes the Grand Alliance High Definition Television (HDTV) standards that have been proposed in the United States. While current video frames consist of the equivalent of 268,800 pixels, systems based on the HDTV standard will be capable of capturing frames with a resolution equivalent to 2,073,600 pixels (1920 x 1080 pixels). High-resolution digital frame cameras will likely become a desirable alternative to video in the near future. Such cameras capable of resolutions in excess of 4 million pixels per frame already exist, and their images can be captured directly into an attached computer (Airola, 1996). Mausel et al. (1992) showed that such a system can provide imagery with resolution similar to that of 70-mm photography.

3. STUDY AREA AND METHODS

3.1 Study Area Description

The pilot study area for this research was selected by the participating researchers and sponsors of the Oregon Biodiversity Conservation Plan for use in a variety of studies aimed at improving livability issues in the Willamette Valley. The Luckiamute and Rickreall watersheds (Figure 1) comprise the chosen study area. These adjacent watersheds are located in the Willamette Valley in western Oregon. The Willamette River forms the eastern boundary of the study area, and the western boundary extends into the Coast Range. The Rickreall watershed (39,713 hectares) is entirely within Polk county while the Luckiamute (81,482 hectares) extends south into Benton county. The eastern portion of the study area, the valley bottom, is predominantly agriculture (mostly grass seed fields and Christmas tree plantations) with smaller areas of white oak woodlands and cottonwood riparian gallery. Young Douglas fir forests dominate the western uplands land cover.

3.2 Data Collection

3.2.1 Landsat TM

The ODFW vegetation map is being created from 23 scenes of Landsat TM data acquired from July 1991 to September 1993 which provide coverage of the entire state at 30 meter resolution. This imagery has already been rectified to the Universal Transverse Mercator (UTM) coordinate system. From these Landsat data, ODFW created a vegetation map of the pilot study area for this study. Additionally, they provided their original, rectified Landsat TM bands covering the study area.

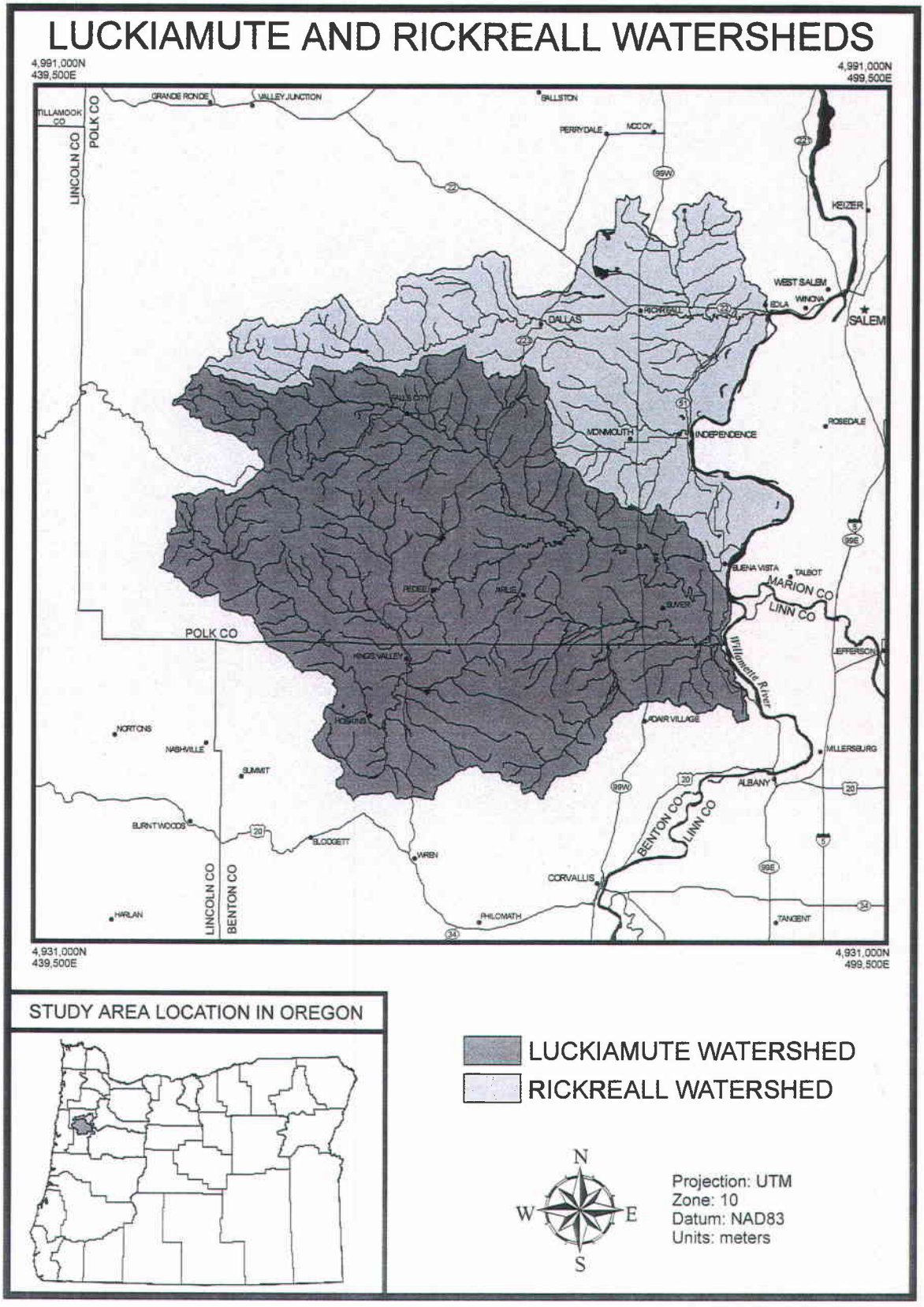

Figure 1: Map of Luckiamute/Rickreall Study Area

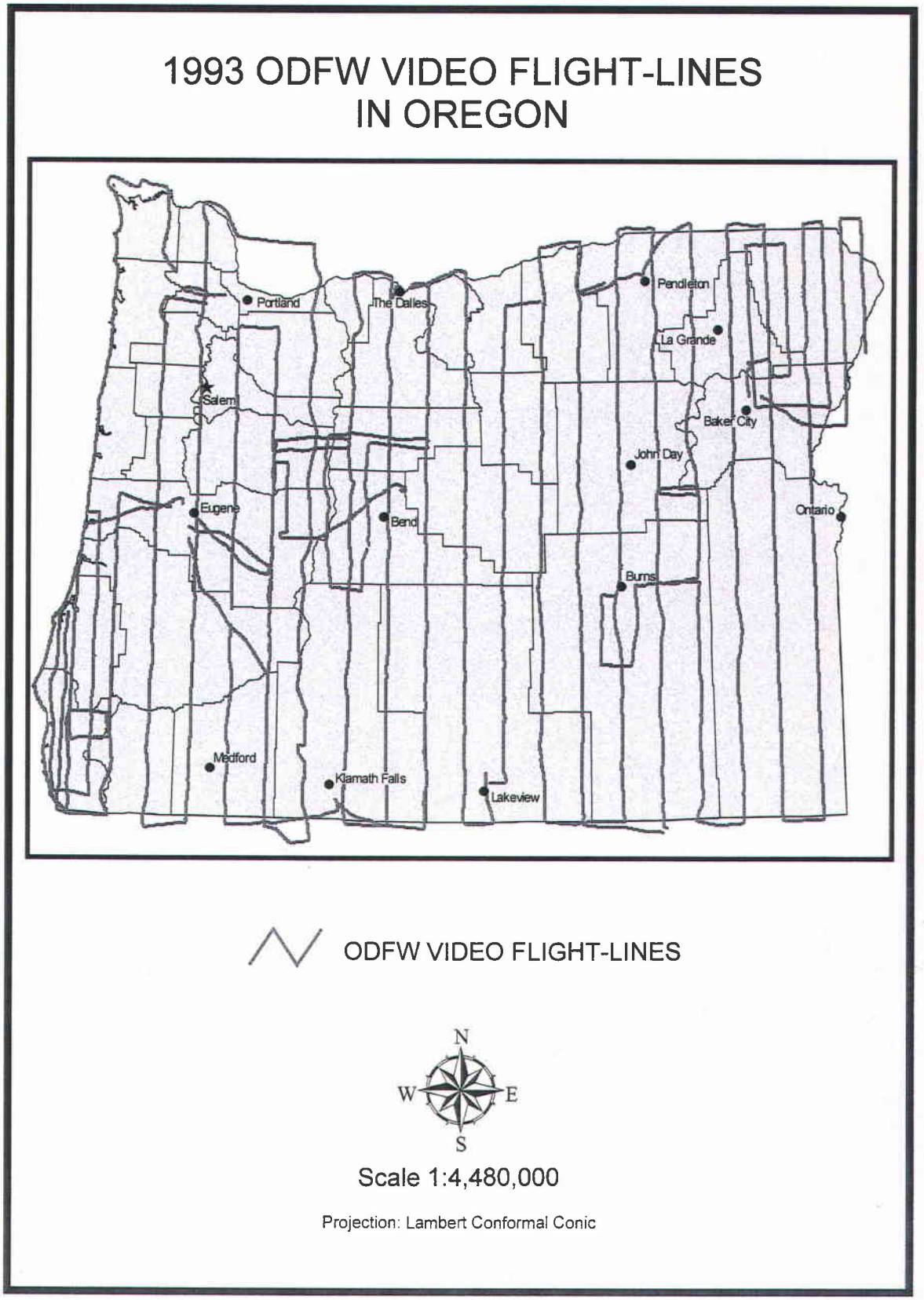

Figure 2: Map of ODFW Video Sampling in Oregon

3.2.2 Airborne Videography

ODFW had airborne videography recorded between August 25 and September 3, 1993. Approximately 4% of Oregon was sampled by flying north-south transects at approximately 30-km intervals (Figure 2). In areas of high vegetation diversity and variability, transects were flown at 15 km intervals. The video was acquired from an airplane flying approximately 600m above the ground with a zoom camera activated every nine seconds for five seconds. Hence, the video has coverage at two scales: approximately 1:1,800 and 1:150 when displayed on a 25 inch diagonal television.

The video acquisition system integrated a digital color video camera, a laptop computer, a Super VHS (S-VHS) VCR a Trimble Pathfinder GPS (Global Positioning System), and a Horita time code generator/recorder/encoder to record real-time location data as well as the video imagery. The Horita time code generator/recorder/encoder recorded the GPS time onto the audio track of the video cassette and dubbed the time in a window directly on the imagery as well. Simultaneously, GPS time and the corresponding location were recorded once per second in a digital file on the laptop computer. At the 1:150 scale, there are more than 18,000 reference points that are GPS geolinked to ground coordinates. These GPS points are not differentially corrected. Therefore, the GPS acquired geodetic measurement could be 0 to 140 meters from the true location of each reference point (Graham 1993).

The Luckiamute and Rickreall watersheds were chosen as the common study area for several related studies comprising the Oregon Biodiversity Conservation Plan. This selected study area, however, was not ideal for this study because ODFW had recorded limited video in these watersheds. In fact, only one of the ODFW video flight-lines intersected the Luckiamute/Rickreall watersheds study area. This flight-line runs north-south along the eastern extents of the Coast Range within the study area. Containing mostly Douglas fir dominated forests and recently harvested forests, this video transect

has limited vegetation variety compared to the study area as a whole. Additionally, much of the area captured in the video was inaccessible for ground verification due to lack of access to private property.

For these reasons, supplemental airborne video was obtained in the study area on August 23, 1996. Three east-west transects were flown at approximately 2,200m above ground level using a single, fixed-lens digital video camera. The Cessna mounted color video acquisition system differed from the ODFW system in that it did not have timed zoom capabilities, the imagery was recorded on Hi8 media instead of S-VHS, and the GPS locations were dubbed on the video instead of the GPS time. The resulting video is slightly smaller-scale (approximately 1:2,400 on a 25 inch diagonal television) than the ODFW pan video, and it contains a more representative sample of the vegetation in the study area. Figure 3 shows the locations of the ODFW and supplemental video transects recorded in the Luckiamute/Rickreall study area.

3.3 Video Processing

Perhaps the greatest challenge of this research was the development of an efficient methodology that permitted the video to be converted to a digital, georeferenced format. This conversion would allow computer analysis of the imagery within a geographic information system (GIS).

The original proposal stated that digitally captured video frames would be matched to the Landsat imagery using the GPS data recorded on the video and a subsequent visual adjustment for each frame. This proposed methodology was to yield a registration accuracy of three Landsat pixels (0 to 90 meters) for the center of each video frame to the Landsat imagery. After capturing test video frames in digital format, it became apparent that there were not enough identifiable features in most of the video frames to successfully match them to the Landsat imagery. Additionally, the small areas

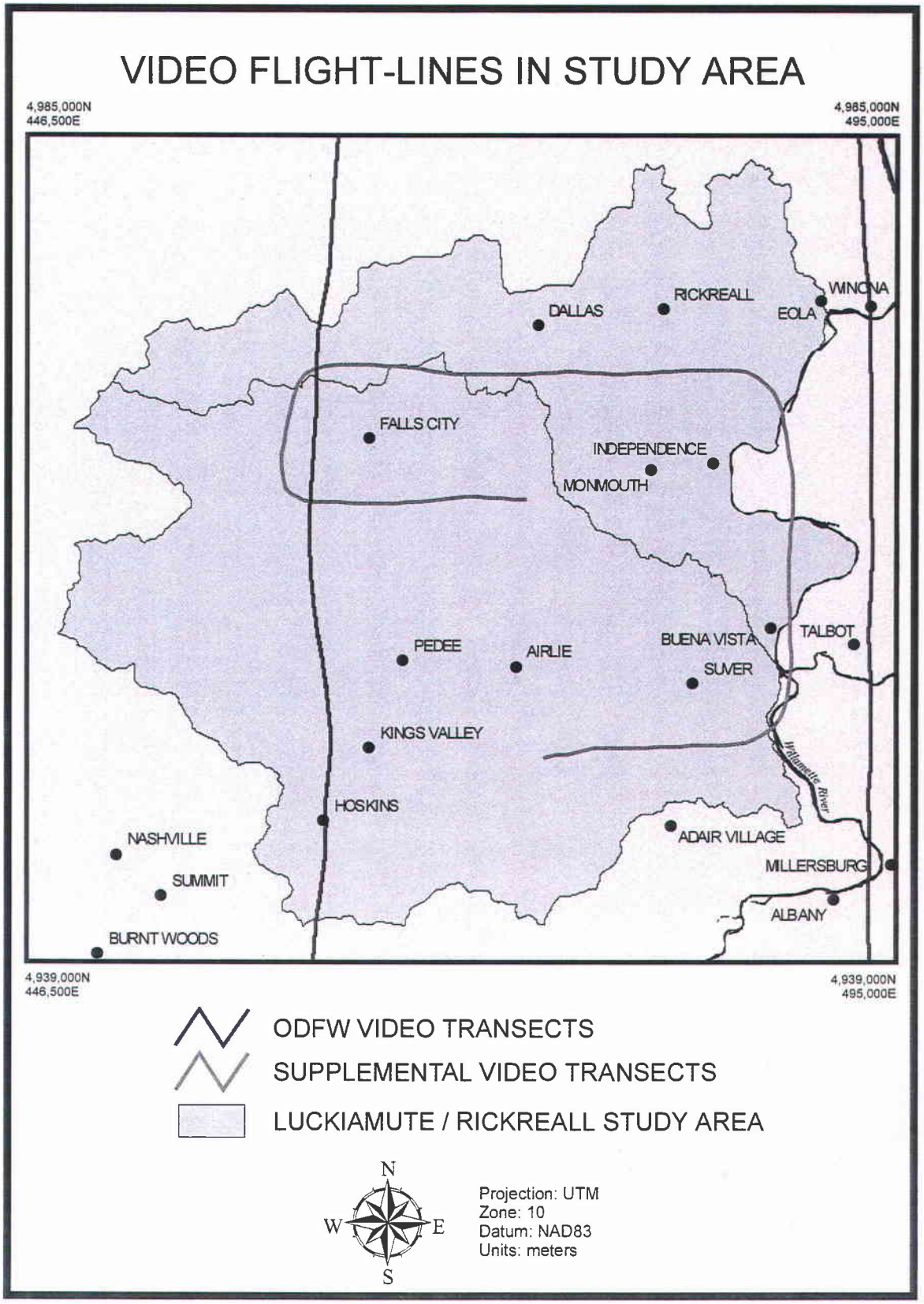

Figure 3: Map of Video Sampling in Study Area

captured in the individual video frames would make it difficult to identify the corresponding ground locations for many of the frames during the ground truth portion of the study.

The underlying problem for both of these obstacles was the small area contained in each video frame. Therefore, it was decided to digitally capture overlapping video frames and mosaic them together using a computer software program. The resulting video frame mosaics provided images containing larger areas that could be georegistered to greater accuracy than the originally proposed method and that could be more easily field-checked. The following section details the procedures used to digitally capture and enhance the video, mosaic the captured video images, and georeference the resulting mosaics.

3.3.1 Video Frame Capture and Enhancement

Video imagery extending slightly beyond the study area boundary was digitally captured using the stock frame-grabber on a UNIX-based Silicon Graphics Indigo (SGI) workstation and IRIS Capture 1.3 software. Several available PC-based frame-grabbers were tested, but none of these yielded near the image quality provided by the SGI system. A S-VHS VCR was attached to the SGI system when capturing the ODFW video, and a Hi-8 camera in playback mode was attached to frame-grab the supplemental videography. From the ODFW video, 120 Overlapping frames were captured at the pan scale and 60 (one every zoom cycle) non-overlapping frames at full zoom. One-hundred twenty-four overlapping frames were captured from the supplemental video. The resulting images were each 640 x 480 pixels with 24-bit color resolution.

In general, the digitally captured video images appeared washed-out. To help compensate for this effect, the Brightness filter in SGI Image Works 2.1 software was applied to each image at the 0.8 setting (Figure 4). These enhanced images were saved in Tagged Image File Format (TIFF) and then ported to a PC for subsequent processing.

Figure 4: Sample Video Image Before and After Brightness Filter

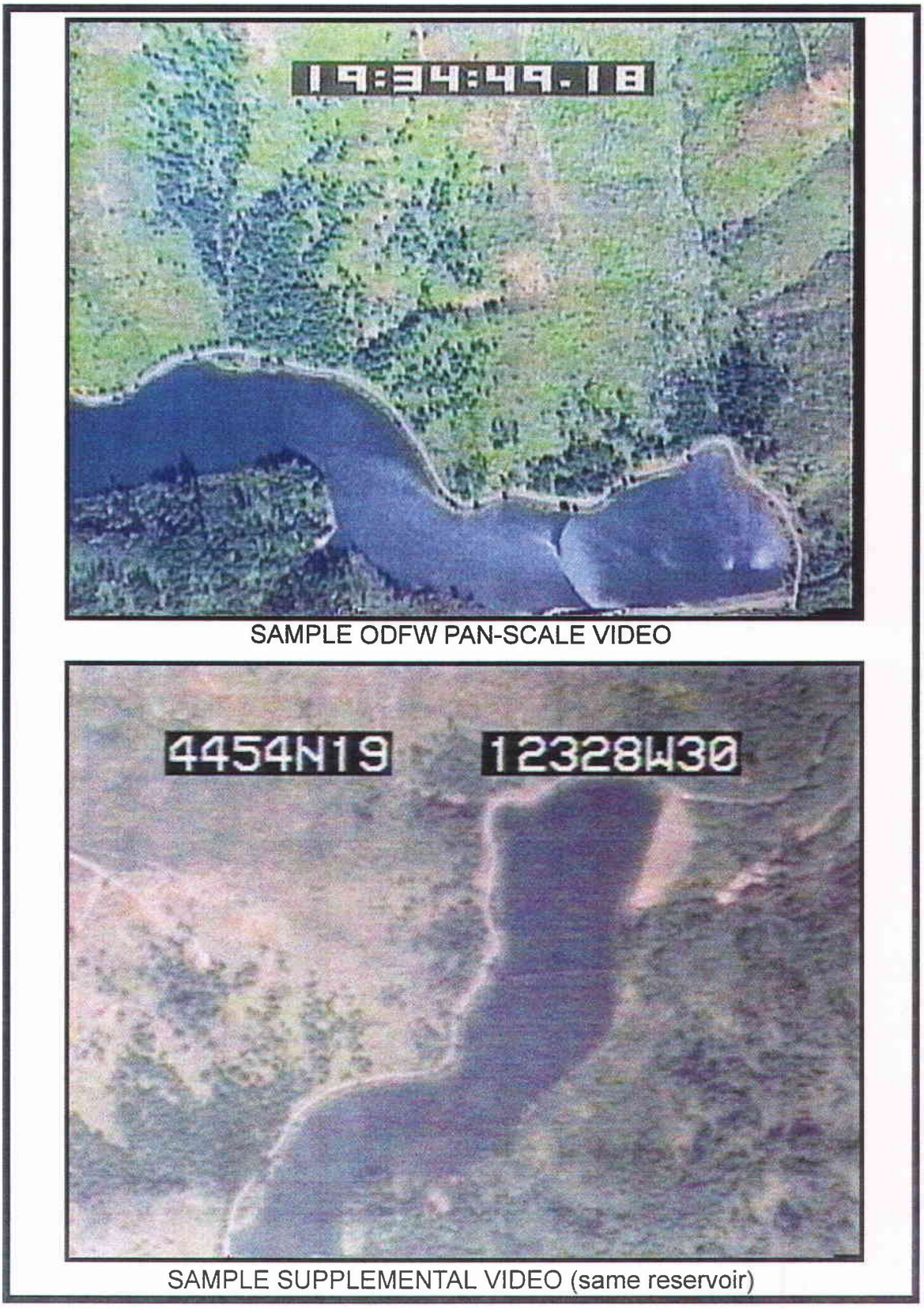

Figure 5: Comparison of ODFW and Supplemental Video

Figure 6: Sample Video Frame Before and After De-Interlace Filter

At this point, it is important to note that the ODFW video had significantly better radiometric resolution than did the supplemental video (Figure 5). This difference was most likely caused by the variation in flight altitude used by each acquisition system more than any other factor. The supplemental video acquisition system was flown at approximately 2200m compared to the 600m altitude used by ODFW. This substantial increase in atmospheric depth between the sensor and earth during the supplemental flight resulted in increased atmospheric scattering, as evidenced by the decreased radiometric resolution of the resulting video.

One other factor that degraded image quality in both the ODFW and the supplemental video was the interlace effect. King (1992), Russ (1995), and Meisner (1986) discussed this potential problem and posed as a solution using a single field in place of a whole frame for analysis. Instead of using single fields for this research, whole frames were captured, and the De-interlace filter in Adobe Photoshop 3.0 software was applied to smooth-out one of the fields. This filter replaces the unwanted field with an interpolated field based on the pixel values of the remaining original field. Figure 6 shows a sample video frame before and after the De-interlace filter application. Most of the images showed a similar, significant increase in sharpness.

3.3.2 Mosaic Video Frames

The ODFW pan-scale and the supplemental video frames were joined to create mosaics (Figure 7) using Adobe Photoshop 3.0. This software allowed sequentially captured digital video frames to be imported as 24-bit TIFF files onto separate layers within one image and then moved, individually or together, as desired. Overlapping edges were then trimmed as much as possible to help eliminate the distortion caused by the video camera optics, which increased toward the edges. This trimming was quickly achieved by simply boxing the undesired areas and deleting them. Next, a common

Figure 7: Sample Mosaic of ODFW Video Frames

point in the center of two video frames' adjacent edges would be found, and the two images would be aligned to that point.

Usually, distortion in the images, from optics and/or aircraft shifts, prohibits the outward extents of the adjacent edges from matching. Therefore, these extents were selected and stretched on both images, splitting the difference of the misalignment between the two images, until the edges matched. Adobe Photoshop contains several distortion filters which allowed this controlled edge alignment. These filters use a resampling algorithm which permit one to distort the selected area more toward the edge and less toward the center of the image. This approach is very reasonable since it basically removes some of the distortion caused by the video acquisition system by resampling the most distorted areas. Limaye et al. (1994) used AutoGCP, a pattern-recognition software program for locating common points in adjacent images, to perform a similar but more automated mosaic process on video of urban areas. However, this software does not work well in forested or agricultural areas (Limaye, personal comm.), so it was not tried in this study.

Between six and eight contiguous video frames were combined to form each mosaic, and three to fifteen of these mosaics comprise a flight-line. The choice of six to eight video frames per mosaic permitted the length of each mosaic to be printed within the constraints of a 36-inch wide plotter at the default 72 pixels per inch (ppi) of the digitally captured video. These 36-inch strips were easily taken into the field, and the larger area contained in these mosaics made it easier to find the corresponding features in the video when field verifying the classification. Additionally, these large areas allowed the mosaics to be efficiently georectified as described in the next section.

3.3.3 Georeference Video Mosaics

Thirty-three mosaics were created from the video captured in and slightly beyond the Luckiamute/Rickreall study area. A preliminary field reconnaissance was conducted

of the areas represented in these mosaics. Only eighteen of these mosaics, six from the ODFW and twelve from the supplemental video, fell within the study area and also contained a majority of area that was ground accessible for subsequent field verification. Therefore, only these eighteen mosaics were selected for rectification to the Landsat imagery which had already been georeferenced to the UTM coordinate system. Portions of the other fifteen mosaics, within and just beyond the study area, were used to develop an interpretation key. This will be discussed in a subsequent section.

Because each mosaic contains a much larger area than the individual video frames, corresponding ground control points (GCPs) from the Landsat imagery could be more easily identified in these images. In fact, there were enough identifiable features to successfully georegister each mosaic to the Landsat imagery using an affine transformation. This procedure involves fitting polynomial equations to control point data using least-squares criteria to model the image distortion corrections (see Jensen, 1986; Richards, 1993). In addition to being a more practical approach to registering the video to the Landsat imagery, this technique helped remove distortions, caused by the camera lens and variations in aircraft attitude and altitude, that were present in the video. It also permitted an estimation of accuracy for each transformation by means of the calculation of a root mean square (RMS) error. A detailed description of the georectification process follows.

Idrisi for Windows software was used to georectify the eighteen mosaics. Since Idrisi only supports up to 8-bit images, each 24-bit mosaic was first split into three 8-bit images, a red, green, and blue band, using Adobe Photoshop. These bands were saved in RAW binary format and then imported into Idrisi where they were rectified individually using the Resample module.

Corresponding GCPs were found in a UTM-georeferenced false-color composite image of the study area, created from Landsat TM bands 2, 3, and 4 (Figure 8), and in a simultaneously displayed green band of each video mosaic. The green band was selected

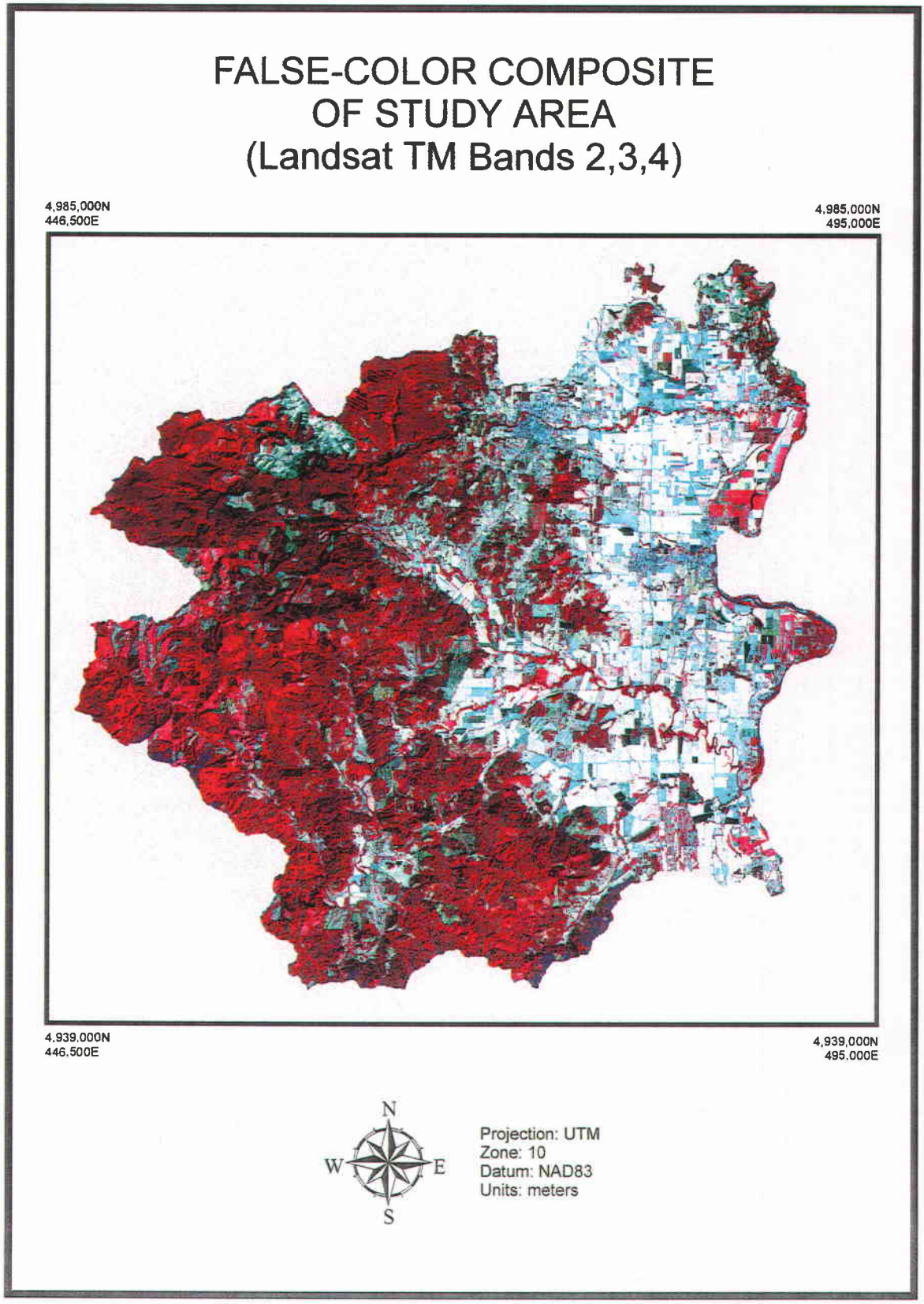

Figure 8: Landsat TM False-Color Composite Map of Study Area

because features (e.g., houses, road intersections, and corners of fields) were easier to visually identify in this band than in the red or blue bands. Between 14 and 22 GCPs, scattered throughout and as far towards the edges as possible, were located in each mosaic, and between 11 and 18 GCPs were retained to develop the polynomial equation used in each transformation. This omission of control points, those that display excessively high residuals when tested in the derived polynomial equation, is a common practice as long as enough control points are preserved to successfully model the transformation (see Jensen, 1986; Richards, 1993). The acceptable minimum number of control points is two to three times the mathematical minimum for the type of equation used, assuming that these control points are well scattered throughout the image. An acceptable minimum number of control points for linear (first order) and quadratic (second order) equations, therefore, is 6 and 12, respectively (Eastman, 1992).

Since it is best to use the lowest order of equation that provides a reasonable fit of the GCPs, a quadratic equation was used only when a linear equation, even after removing several high-residual GCPs, resulted in a very high RMS error. The need for the use of a quadratic equation in all of the ODFW video mosaics resulted from excessive lens distortion (due to a wider angle lens) and the highly varied elevations in the Coast Range mountains recorded in the ODFW video transect. In three of the supplemental video mosaics, the quadratic equation was applied to remove distortions caused when the aircraft was beginning or ending slightly banked turns. Cell values in all transformed images were interpolated using a nearest neighbor interpolation whereby the value of the closest input cell was transferred to the position of the output cell.

The final georectified video mosaic bands were resampled to two resolutions. The transformed cell size was kept as close as possible to the average cell size in the input images to preserve image quality and to still be able to print the length of each mosaic within the 36 inch width of the available plotter. Additionally, an odd-sized cell was not desired. The solution was to resample the ODFW video to 1.5 meter per side

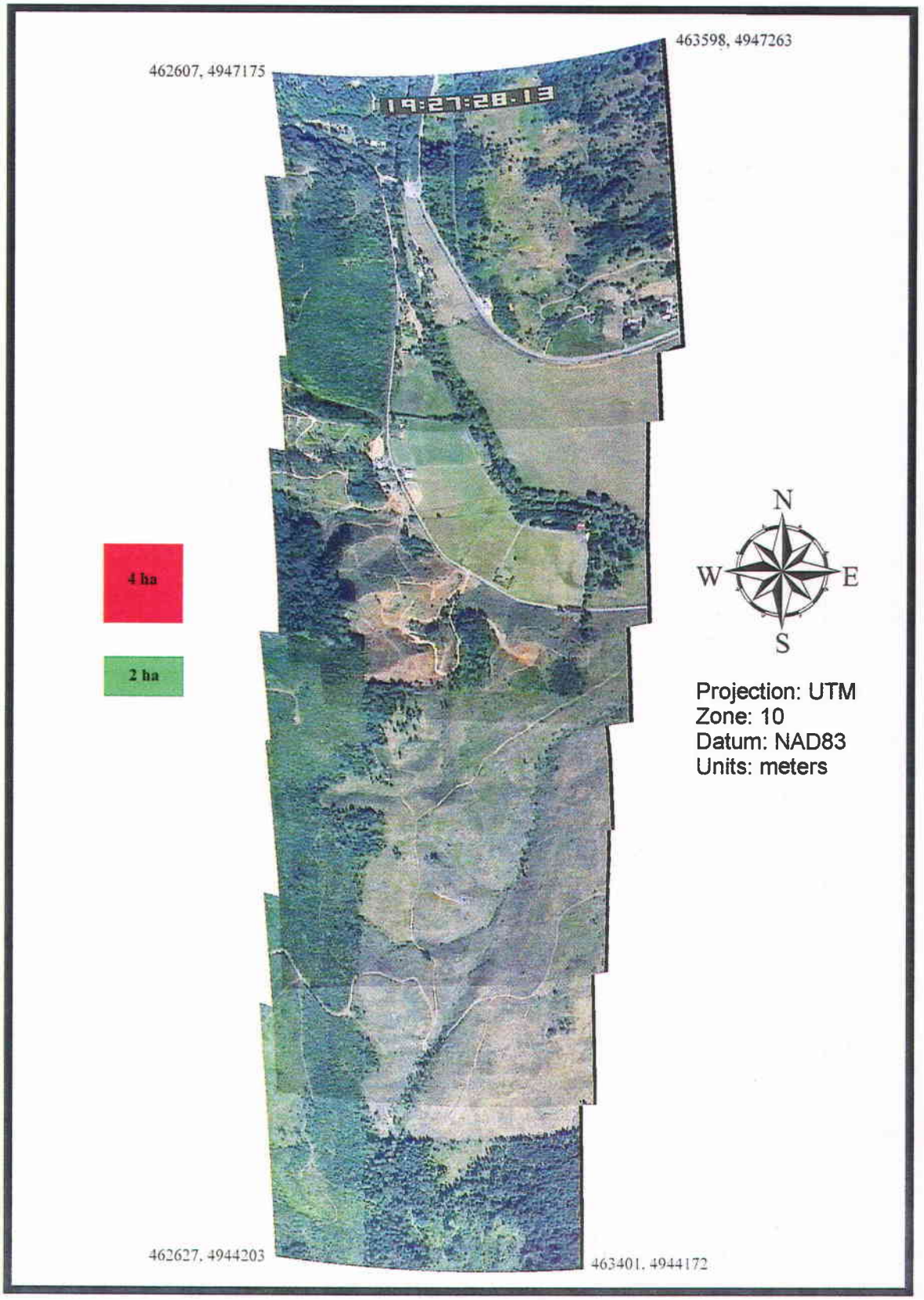

Figure 9: Sample Georectified Mosaic of ODFW Video Frames

(2.25m^2) cells and the supplemental video to 2 meter per side (4m^2) cells. When subsequently printed on the plotter at 72ppi, the resulting images were slightly smaller than the non-rectified mosaics at scales of 1:4,250 and 1:5,670, respectively. Prior to printing, however, all three georectified bands of each mosaic had to be exported back to Adobe Photoshop as RAW images and recombined into 24-bit true color images. Additionally, at least four tic marks were determined in each mosaic using Idrisi for Windows and then located on the final mosaics for use in subsequent processing. Figure 9 shows the same mosaic from Figure 7 after the georectification process.

MOSAIC NAME	POLYNOMIAL EQUATION TYPE	NUMBER OF CONTROL POINTS IDENTIFIED	NUMBER OF CONTROL POINTS RETAINED	ESTIMATED RMS (pixels)	ESTIMATED RMS (meters)	FINAL IMAGE RESOLUTION (meters)
ODFW-1	quadratic	18	16	11.698	16.38	1.5
ODFW-2	quadratic	19	14	13.848	19.39	1.5
ODFW-3	quadratic	19	18	14.863	20.81	1.5
ODFW-4	quadratic	18	15	10.633	14.89	1.5
ODFW-5	quadratic	17	14	15.942	22.32	1.5
ODFW-6	quadratic	19	16	11.596	16.23	1.5
SUPPLEMENTAL-1	linear	17	14	12.327	21.57	2
SUPPLEMENTAL-2	linear	16	14	12.147	21.26	2
SUPPLEMENTAL-3	linear	18	14	9.65	16.89	2
SUPPLEMENTAL-4	linear	18	16	8.157	14.28	2
SUPPLEMENTAL-5	linear	20	16	7.107	12.44	2
SUPPLEMENTAL-6	linear	20	16	8.556	14.97	2
SUPPLEMENTAL-7	linear	20	17	8.6	15.05	2
SUPPLEMENTAL-8	quadratic	22	20	10.843	18.98	2
SUPPLEMENTAL-9	quadratic	19	18	8.58	15.02	2
SUPPLEMENTAL-10	quadratic	19	17	10.37	18.15	2
SUPPLEMENTAL-11	linear	15	12	10.017	17.53	2
SUPPLEMENTAL-12	linear	15	11	14.909	26.09	2

Table 1: Summary of Polynomial Transformations for Georectified Mosaics

Table 1 summarizes the transformations used to rectify the three bands of each mosaic. The resulting RMS errors suggest that any point on a georegistered, mosaiced image using this methodology will match the Landsat imagery to within two Landsat pixels (0 to 60 meters) and in many cases one pixel (0 to 30 meters). Subsequent observations when joining adjacent mosaics (described later), however, suggest that the error near the edges of some mosaics may approach 90 meters. This is not surprising given that it was impossible to identify control points along many of the mosaics' edges.

The originally proposed methodology aimed for a match of within three Landsat pixels (0 to 90 meters) for the center point only of each video frame and would not have removed any distortion in the video. Location inaccuracies toward the edges of each frame using that method would likely be much greater than 90 meters. Therefore, the resulting level of accuracy was considered acceptable and a substantial improvement over the originally proposed visual-adjustment method.

3.4 Classification Systems

Two vegetation classification systems were used in this study. The first system was developed by the ODFW researchers who created the Landsat-based vegetation map of the study area. Their scheme followed the approach suggested by O'Neil et al. (1995) and crosswalks to the current Gap analysis vegetative groupings that list 133 types (Kagan and Caico, 1992). Figure 10 shows the ODFW vegetation classification system being used for the Landsat-based vegetation map of Oregon. The classes in bold are those potentially occurring in the Luckiamute/Rickreall watersheds. The second classification system (Figure 11) was developed during this study to compare the manually interpreted video to the field verified video at a 1hectare minimum mapping unit (MMU). To better test the limitations of manual interpretation from airborne videography, this classification system was adopted instead of using the ODFW vegetation classes. It was derived from a combination of observed vegetation types during a preliminary field reconnaissance, the classification used by ODFW's Willamette Valley Habitat Mapping Project, and the ODFW classification scheme already mentioned. This video classification system was subsequently nested into the ODFW scheme (Figure 12) to complete the accuracy assessment of their Landsat-based vegetation map.

ODFW's Vegetation Classes for Oregon

1. Sitka Spruce/Willow Palustrine Forest
2. Maritime Mixed Conifer
3. Mountain Hemlock
4. True Fir/Hemlock Forest
5. Montane Mixed Conifer
6. Siskiyou Montane Conifer Forest
7. Whitebark - Lodgepole Pine Forest
8. East Cascade-Sierran Mixed Conifer Forest
9. Northeastern Oregon Mixed Conifer Forest
10. Jeffery Pine Forest and Woodland
11. Serpentine Woodland
12. Lodgepole Pine Forest
13. Subalpine Fir - Lodgepole Montane Forest
14. Coastal Lodgepole
15. **Douglas Fir Forest**
16. **Douglas Fir/Western Hemlock/Western Red Cedar Forest**
17. Douglas Fir/Mixed Deciduous
18. Douglas Fir/Tanoak/Madrone
19. **Douglas Fir/White Oak**
20. Ponderosa Pine Forest and Woodland
21. Ponderosa Pine/Douglas Fir/Incense Cedar Forest
22. Ponderosa Pine/Oregon White Oak Forest
23. Ponderosa Pine/Western Juniper Woodland
24. Ponderosa Pine/Lodgepole Pine Woodlands on Pumice
25. Western Juniper Woodland
26. **Red Alder Forest**
27. **Red Alder/Bigleaf Maple Forest**
28. **Red Alder/ Cottonwood Riparian Gallery Forest**
29. Aspen Groves
30. **Red Alder/Conifer**
31. **Cottonwood Riparian Gallery**
32. Siskiyou Mixed Deciduous
33. **Oregon White Oak Forest**
34. Alpine Mixed Conifer
35. South Coast Mixed Deciduous
36. Canyon Shrubland
37. **Hawthorn-Willow**
38. Alpine Shrubland
39. Manzanita Shrubland
40. Mountain Mahogany Shrubland
41. Sage/Grass Mosaic
42. Mixed Sage
43. Low Sage
44. Coastal Shrublands
45. Salt Desert Scrub
46. Big Sage
47. Bitterbrush/Big Sage
48. Willow Riparian
49. Eastside Riparian (Alder Dominant)
50. Palustrine Shrub
51. Northeast Oregon Canyon Grasslands
52. Montane Grassland
53. Forest-Grass Mosaic
54. Great Basin Grassland
55. Coastal Headland Grassland
56. Alpine Parkland
57. Alkali Wetlands and Grasslands
58. Modified Grassland
59. Coastal Strand
60. Wet Meadow
61. **Shrub Dominant**
62. Alkali Playa
63. **Urban**
64. **Agriculture**
65. **Bare Ground**
66. Lava Flow
67. Dunes
68. Rock/Snow/Ice
69. **Open Water**
70. **Palustrine Forest**
71. **Palustrine Shrub**
72. Estuarine Emergent
73. **Palustrine Emergent**

** Classes in **bold** indicate those possible in study area.*

Figure 10: ODFW Classification for Vegetation Map of Oregon

Video Classification System at 1ha MMU

1. **Douglas Fir**
   > 65% Douglas fir
2. **Douglas Fir / Western Hemlock - Western Red Cedar**
   approximately 50 ·70% Douglas fir and approximately 30% western hemlock and or red cedar
3. **Douglas Fir / Red Alder / Bigleaf Maple**
   < 65% Douglas fir with bigleaf maple and/or red alder > 33% (Usually Douglas fir dominant)
4. **Douglas Fir / Oregon White Oak**
   < 65% Douglas fir and >33% Oregon white oak
5. **Red Alder**
   > 65% red alder
6. **Red Alder / Bigleaf Maple**
   < 65% red alder and >33% bigleaf maple
7. **Oregon Ash / Black Cottonwood / Bigleaf Maple**
   approximately 33% of each specie; may only contain two of the three species, but the dominant specie will be < 65%; may occasionally contain < 33% willow
8. **Oak Forest**
   > 65% Oregon white oak (Balance usually Douglas fir or bigleaf maple); >30% canopy cover
9. **Oak Woodland**
   > 65% Oregon white oak; 10·30% canopy cover
10. **Oregon White Oak / Douglas fir - Bigleaf Maple**
    < 65% Oregon white oak > 50%; approx. 30% Douglas fir and/or bigleaf maple; >30% canopy
11. **Shrub / Seed / Sapling**
    includes recent clear cuts through pole-sized forests
12. **Black Hawthorn**
    includes most hedgerows; may also be abandoned pasture where Black Hawthorne, along with apple and cherry trees and/or berries, have intruded to cover >65% of a field.
13. **Scotchbroom**
    > 65% Scotchbroom
14. **Willow**
    > 65% willow of various species
15. **Herbaceous Riparian**
    wetlands or seasonally wet areas characterized by tufted hairgrass, reed canarygrass, carex spp., and/or douglas spiraea
16. **Cropland and Pasture**
17. **Orchards, Groves, Vineyards, Nurseries and Ornamental Horticultural Areas**
18. **Christmas Tree Plantations**
19. **Cottonwood Plantations**
20. **Residential**
21. **Open Water**
22. **Unclassified (inaccessible)**

Figure 11: Video Classification System at 1 Hectare MMU

Nesting of Video Classification into ODFW's Classification System

Douglas Fir Forest
1-Douglas Fir

Douglas Fir/Western Hemlock/Western Red Cedar Forest
2-Douglas Fir/Western Hemlock-Western Red Cedar

Douglas Fir/White Oak
4-Douglas Fir/Oregon White Oak
10-Oregon White Oak/Douglas Fir - Bigleaf Maple

Red Alder Forest
5-Red Alder

Red Alder/Bigleaf Maple Forest
6-Red Alder/Bigleaf Maple

Red Alder/Conifer
3-Douglas Fir/Red Alder/Bigleaf Maple

Cottonwood Riparian Gallery
7-Oregon Ash/Black Cottonwood/Bigleaf Maple

Oregon White Oak Forest
8-Oak Forest
9-Oak Woodland

Willow-Hawthorn
14-Willow
12-Black Hawthorn

Palustrine Emergent
15-Herbaceous Riparian

Shrub-Dominant
11-Shrub/Seed/Sapling
13-Scotchbroom

Agriculture
16-Cropland and Pasture
17-Orchards, Groves, Vineyards, Nurseries and Ornamental Horticultural Areas
18-Christmas Tree Plantations
19-Cottonwood Plantations

Open Water
21-Open Water

ODFW's classes are in **bold.*

Figure 12: Nesting Method for Video Classification into ODFW's Classification

3.5 Videography Manual Interpretation Techniques

The airborne videography for the pilot study area was visually interpreted using manual techniques and guides such as those discussed by Avery and Berlin (1992) and Sayn-Wittgenstein (1978). Knowledge of ground appearance gained through a preliminary field reconnaissance in the pilot study area and of areas adjacent to the study area (i.e., areas contained in the fifteen non-georeferenced video mosaics) supplemented these techniques. Portions of the non-study area video mosaics containing areas that could be ground accessed were field-interpreted and used as an interpretation key. This selective key was used to help manually interpret the georeferenced video mosaics.

A multiple step process was used to interpret the video mosaics. As stated previously, the scale of the printed mosaics was 1:4,250 for the ODFW and 1:5,670 for the supplemental video. To aid the interpretation of these mosaics, the video was simultaneously displayed on a 25-inch color television at the scales of 1:1,800 and 1:2,400, respectively. For the ODFW video, the availability of the 1:150 zoomed video aided the interpretation immensely (see Figure 13). The video was classified to 1ha minimum polygons which were drawn onto mylar overlays aligned over each printed mosaic using established control points. A 1ha MMU was chosen because that appeared to be the smallest area that could be universally identified in the video given any location and its corresponding classification. For example, a less than 1ha cluster of Douglas fir could be easily identified when surrounded by agricultural pasture, but this same polygon would probably not be distinguished if surrounded by 10ha of Douglas fir / Maple - Alder forest.

After the interpretation, these polygons were digitized into a vector format using the Arc Edit module of ARC/INFO. Adjacent mosaics were joined also with ARC/INFO. This process revealed that the location difference between the same point near the edges of two adjacent mosaics could be as much as 90 meters as a result of the image

rectification process described previously. Finally, the digitized polygons were attributed using ArcView 3.0. The UTM coordinate system was preserved in this raster-to-vector conversion process.

Avery and Berlin (1992) described eight commonly used recognition elements in airphoto interpretation which include shape, size, pattern, shadow, tone or color, texture, association, and site. Color, texture, shape, and site were found to be the most helpful of these elements in the manual interpretation of the video. However, interpretation was not easy due to color and texture differences within vegetation classes in the video, especially in the supplemental video. An a priori knowledge of the study area's vegetation combined with analysis of the questioned feature's site was perhaps the most useful factor for interpreting the supplemental video. Shadow and shape became significant recognition elements when using the much larger-scale zoomed video to help interpret the ODFW video because conifer and deciduous trees could be more confidently distinguished by their shadows.

3.6 Videography Field Verification

The printed video mosaics were taken to the field for classification verification. The initial field-interpretation occurred in October 1996, and a subsequent verification of questionable areas was performed the last week in March 1997. All the accessible areas contained in each mosaic were classified using a 1hectare MMU to correspond to the MMU used in the manual video interpretation. Areas that could not be verified were labeled "not accessible" and subsequently omitted from the analysis.

These field-gathered data were subsequently entered into ARC/INFO. To help eliminate polygon delineation and digitizing error from being introduced into the subsequent analysis, the polygon coverage from the manually interpreted video was used as the starting point instead of digitizing all of the field-classified mosaics. Polygons identified in both interpretations were preserved. Polygons in the manual interpretation

but not identified in the field were eliminated, and those from the field and not in the manual interpretation were added. The polygons in the resulting coverage were then attributed with the appropriate field-interpreted classes using ArcView software.

It should be noted that the use of a pen computer with Field Notes software was originally proposed to help automate the field data collection in this research. After careful evaluation, however, it was determined that this approach would be less efficient than the adopted method. Four major problems existed. First, the image resolution on the pen computer would not be acceptable for distinguishing vegetation transition zones on the video imagery. The 24-bit mosaics would have to be decreased to inferior 256-color 8-bit images as required by the Field Notes software. Additionally, the only pen computer available for this research had a gray-scale display, not color. Second, the large size of each mosaic, approximately 3 megabytes at 8-bit resolution, would lead to slow and tedious display refreshes when changing views on the available 486SX-33mhz pen computer. Third, the process of drawing and labeling polygons in the field with Field Notes software was determined to be inefficient. Field-collected data using this software would have required substantial post-processing to close polygons and to get the data into a useable format. Finally, the location accuracy of polygons resulting from on-screen digitizing, over a poor resolution image and digitized while in the field, would have been less accurate than those digitized using the adopted method.

3.7 Sampling Strategies

The ODFW video was acquired using a systematic random transect sampling scheme covering the entire state of Oregon. Approximately 4% of Oregon was sampled with north-south transects recorded at 30km intervals. If the vegetation map being produced for the entire state of Oregon were being assessed for accuracy, point samples would have been taken along these transects every time the video zoomed. Since there are in excess of 18,000 zooms, a sufficient number of sample points could be obtained in

this manner to statistically assess the accuracy of the Oregon vegetation map for many but not all of the vegetation classes. Additionally, the zoomed imagery provides much higher spatial resolution than the panned video (Figure 13), and therefore, zoomed samples would be more easily and accurately interpreted.

With the selection of the Luckiamute and Rickreall watersheds as the pilot study area, two significant problems arose in this research. First, the single ODFW video transect recorded in this study area recorded only upland vegetation which does not adequately represent the vegetation found in the study area. Second, this single transect did not have enough zooms to use the zoom-point sampling method. Therefore, the supplemental video, consisting of three random east-to-west transects without zooms, was acquired, and a new strategy had to be developed to sample and assess the vegetation map of the pilot study area. The supplemental transects were flown east-to-west capturing the landscape transition from valley bottom to Coast Range foothills and, therefore, the highest possible variety of vegetation types.

The new sampling strategy included using both the ODFW video and the supplemental video. As previously described, both sources of video were digitally captured and mosaiced. Only the mosaics that could be field verified were selected to be georeferenced and used for the subsequent analysis (Figure 14). These mosaics sampled 5.28 percent (6,404 hectares) of the study area.

According to traditional statistical methods assuming normally distributed data, approximately 256 pixels per classification type would have to be sampled to achieve the desired map classification accuracy rate of 80% with a standard error of 2.5% (Hay 1979; F. Ramsey, Oregon State University, personal comm.). Congalton (1996) emphasized, however, that traditional methods are not appropriate for determining the sample size when using an error matrix, and furthermore, traditional thinking about sampling usually does not apply to remotely sensed data because of the large number of pixels in an image. Additionally, he argued that remotely sensed data are usually not normally distributed

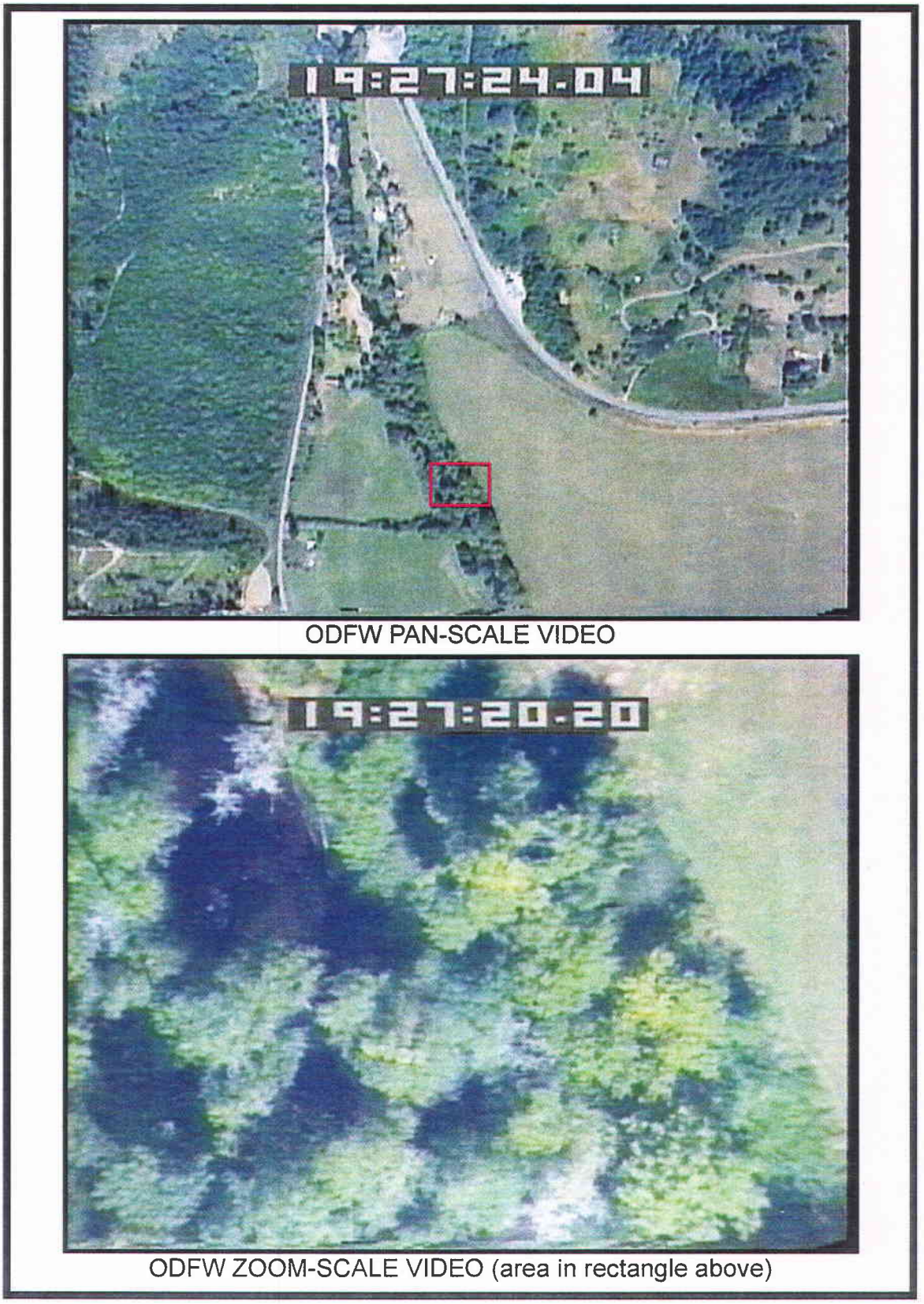

Figure 13: Comparison of ODFW Pan-Scale Video to Zoom-Scale Video

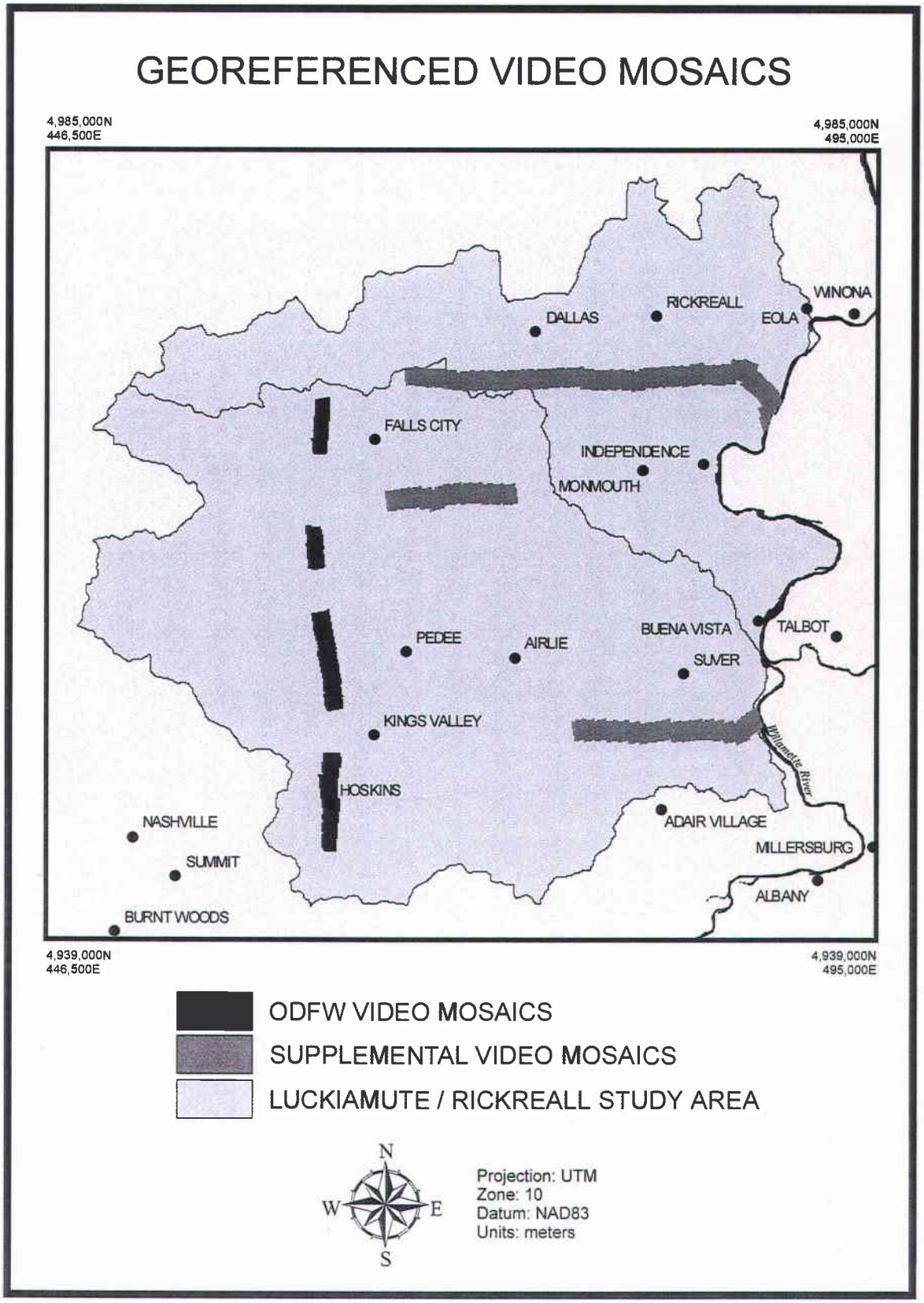

Figure 14: Map of Georeferenced Video Mosaics

(see Chapter 1). His experience suggests that if the area being sampled is larger than a million acres or the classification has more than 12 categories, the minimum number of samples should be 75 to 100 samples per category. For smaller areas with less than 12 categories, a minimum of 50 samples per category would suffice.

Given the small amount of videography sample data available for the study area, the violation of the assumption of sample independence and the related negative effects of spatial autocorrelation were problems with any analysis method considered. The spatial autocorrelation effect described in Chapter 1 suggests that the value of a pixel is affected by other pixels within close proximity of it. Generating enough random points to have even 50 samples per class resulted in multiple samples in almost every polygon. Therefore, any statistical inferences made from the data acknowledge this sample independence shortcoming. The ideal solution would have been to have many systematic random transects of the study area flown with a zoomed camera to generate a point sampling of sufficient size for analysis. However, funding was not available to acquire such data.

Acknowledging the existence of the spatial autocorrelation effect and the lack of sample independence, two comparisons were performed. First the manually interpreted ODFW and supplemental video were compared to the field classifications of the corresponding areas. This analysis would help determine the extent to which airborne videography might replace field work. Due to the limited amount of georeferenced data available for the study area and the large number of classes (21), it was decided to use all of the georeferenced mosaics, with every pixel as a sample unit, in this analysis. This yielded a more descriptive class-by-class analysis than generating random points. However, the inequality in class sizes using the "every pixel" method resulted in very suspect overall accuracy statistics. To improve the accuracy of this statistic, 75 random points for each class occupying more than 50 acres and/or 2 polygons were subsequently generated with Erdas Imagine and analyzed for both the ODFW and supplemental video.

This equalized random sample would give each class equal weight in the overall accuracy statistic regardless of class size. The smaller classes were dropped in this part of the analysis to help reduce error caused by the lack of sample independence.

The second analysis performed in this research evaluated the classification accuracy of the Landsat-based vegetation map produced by ODFW using the field classified video mosaics. Since there were fewer classes represented in the ODFW classification, an equalized random sample of 50 points per class was created and evaluated. However, it should be noted that there were still multiple sample points in many classified polygons.

3.8 Error Matrices Development

3.8.1 Manually Interpreted Compared to Field-Verified Video

Two error matrices, one for the ODFW and one for the supplemental video mosaics, were developed, using Idrisi software, to assess the classification accuracy of the manually interpreted video on a pixel-by-pixel basis. These matrices compare the 1ha MMU manually interpreted video mosaics to the 1ha MMU field-interpreted video mosaics. Before the error matrices could be generated, however, the vector-format classifications were converted back to a raster format with the original grid-cell sizes of $1.5m^2$ and $2m^2$ for the ODFW and supplemental video, respectively. Error matrices containing column and row marginal totals, errors of omission and commission, and overall error measures were then calculated for both data sets.

Two additional error matrices, one for the ODFW and one for the supplemental video mosaics, were developed in a similar manner to derive a more robust estimate of overall accuracy. These matrices, however, compare 75 randomly generated points for each class greater than 50 acres and/or with more than 2 polygons in the manual video

interpretations to their corresponding points in the field classified mosaics. These equalized random points were generated in Erdas Imagine prior to being imported into Idrisi.

3.8.2 Field-Verified Video Compared to Landsat-Based Map

To assess the accuracy of the Landsat TM-based vegetation map developed by ODFW, two error matrices were generated. First, the field-verified video mosaics were reclassified into the ODFW classification so that they could be compared to the vegetation map. The resulting data were then converted in ARC/INFO from a 1hectare MMU to a 4 hectare MMU to match the ODFW vegetation map MMU. The resulting data were then converted to a raster format with a $30m^2$ grid cell to correspond to the Landsat-based vegetation map of the study area. An equalized random sample of 50 points per class was then generated for the ODFW Landsat-based vegetation map. The first error matrix was then generated to compare the random sample points from the Landsat-based vegetation map to the 4 hectare MMU field verified video classification. A second error matrix was developed that compensated for georectification errors that occurred between the two data sets. Again, each error matrix included column and row marginal totals, errors of omission and commission, and overall error measures.

4. RESULTS

4.1 Evaluation of Manually Interpreted Video

Four error matrices were developed to evaluate the accuracy of the manually interpreted airborne video. Tables 2 and 3 contain error matrices depicting pixel-to-pixel comparisons of the manually interpreted ODFW and supplemental video to the field classified video. The error matrices in Tables 4 and 5 evaluate an equalized random point sample of the video classifications. This section details and explains these error matrices.

4.1.1 ODFW Video

The overall accuracy recorded in Tables 2 and 3 is very similar. The manually interpreted ODFW video yielded an overall accuracy of 89.5% while the supplemental video had an overall accuracy of 87.43%. This small difference in overall accuracy is quite surprising given the better clarity of the ODFW video than the supplemental video as well as the availability of the larger-scale zoomed video for the ODFW video interpretation. A closer look at each matrix explains this similarity in overall accuracy and highlights the need to look further than overall accuracy when evaluating these video classifications.

Table 2 shows that only 12 classes were represented in the ODFW video samples of the Luckiamute and Rickreall watersheds. Of these twelve classes, three, Douglas Fir, Shrub / Seed / Sapling, and Douglas Fir / Red Alder / Bigleaf Maple, comprised almost 83% of the total area sampled in the video. Within these major classes, the greatest source of confusion was between Douglas Fir and Douglas Fir / Red Alder / Bigleaf Maple. Approximately 33% of the vegetation labeled Douglas Fir / Red Alder / Bigleaf Maple in the video interpretation was actually Douglas Fir. Looking at this

Table 2: ODFW Video-to-Field Classification Error Matrix

Field / *ODFW Video*	Douglas Fir	Douglas Fir / Western Hemlock / Western Red Cedar	Douglas Fir / Red Alder / Bigleaf Maple	Red Alder	Red Alder / Bigleaf Maple	Oregon Ash / Black Cottonwood / Bigleaf Maple	Shrub / Seed / Sapling	Scotchbroom	Cropland and Pasture	Christmas Tree Plantations	Residential	Open Water	TOTAL	ERRORS OF COMMISSION (proportional)
Douglas Fir	1,932,723	31,592	17,479	0	14,042	0	0	1	2	0	2	0	1,995,841	0.0316
Douglas Fir/ Western Hemlock / Western Red Cedar	0	0	0	0	0	0	0	0	0	0	0	0	0	0.0000
Douglas Fir / Red Alder / Bigleaf Maple	629,010	0	1,293,083	0	0	0	0	0	3	0	0	0	1,922,096	0.3273
Red Alder	0	0	0	8,836	0	0	0	0	0	0	0	0	8,836	0.0000
Red Alder / Bigleaf Maple	0	0	0	0	246,195	0	0	0	0	0	0	0	246,195	0.0000
Oregon Ash / Black Cottonwood / Bigleaf Maple	0	0	0	0	0	32,186	0	0	0	0	0	0	32,186	0.0000
Shrub / Seed / Sapling	4	0	9,857	0	5,438	0	2,020,642	18,043	0	0	6,302	0	2,060,286	0.0192
Scotchbroom	0	0	0	0	0	0	0	0	0	0	0	0	0	0.0000
Cropland and Pasture	0	0	0	0	0	0	0	6,833	423,734	7	2,628	0	433,202	0.0219
Christmas Tree Plantations	0	0	6,366	0	0	0	0	0	1	434,925	0	0	441,292	0.0144
Residential	0	0	0	0	0	0	0	0	0	0	0	0	0	0.0000
Open Water	0	0	0	0	0	0	0	0	0	0	0	4,378	4,378	0.0000
TOTAL	2,561,737	31,592	1,326,785	8,836	265,675	32,186	2,020,642	24,877	423,740	434,932	8,932	4,378	7,144,312	
ERRORS OF OMISSION (proportional)	0.2455	1.0000	0.0254	0.0000	0.0733	0.0000	0.0000	1.0000	0.0000	0.0000	1.0000	0.0000		*0.1046*

OVERALL ACCURACY: **89.54%**

misclassification from the perspective of omission error, about 25% of the actual Douglas Fir was mistaken for Douglas Fir / Red Alder / Bigleaf Maple. In most instances, the primary cause of these misclassifications was the inability of the video interpreter to accurately estimate the percentage of red alder and bigleaf maple mixed with Douglas fir. Often, the amount of alder and maple was over-estimated in these cases. Another factor causing this confusion was fuzzy classification error or "fuzziness" between classes. That is, when doing the field mapping, there were many times when deciding whether an area was greater than or less than 65% Douglas fir was subjective. In younger stands, this distinction was easier because the maples and alders were generally as tall or taller than the Douglas fir. However, in more mature stands, the Douglas fir were taller than the maples and alders in the canopy gaps. The video allowed the interpreter to see more of the alders and maples that in the field were being concealed from sight by the taller Douglas fir. Therefore, the presence of alder and maple was over-emphasized in the video interpretation and possibly under-emphasized in the field interpretation.

Table 2 also highlights that three classes were totally missed in the ODFW video interpretation. The one stand of Douglas Fir / Western Hemlock / Western Red Cedar occurring in the video sample was inappropriately classified as Douglas Fir. This stand was observed during the video interpretation as having a slightly darker color and coarser texture than the surrounding Douglas fir. However, it occurred near the edge of a mosaic, and no zoomed video was available of it to help with the interpretation. The assumption was incorrectly made that it was an older stand of Douglas fir. Had zoomed video been available for this area or if there had been more occurrences of this class in the video, a correct video interpretation would have likely resulted. The other two classes that were missed in the video were Residential and Scotchbroom. The residential occurrences were mislabeled twice as Shrub / Seed / Sapling and once as Cropland and Pasture. All three of these instances were cases where the field interpretation could have

gone either way. That is, how much development is required for an area to be called Residential as opposed to Agricultural or Shrub / Seed / Sapling? Likewise, the instances where Scotchbroom was identified in the field could have arguably been correctly labeled Shrub / Seed / Sapling or Cropland and Pasture as it was labeled in the video interpretation. Interpreter subjectivity and the decision during the field interpretation (after the video interpretation was complete) to make scotchbroom its own class caused these disagreements in classifications.

4.1.2 Supplemental Video

Table 3 contains the error matrix of the supplemental video interpretation compared to the field interpretation. As mentioned earlier, the area covered by this video sample was predominantly in the valley areas whereas the area covered by the ODFW video was in the Coast Range. Therefore, the greater number and variety of classes observed in this error matrix was anticipated. The high overall accuracy of 87.43% is surprising, however, given that no zoomed video was available in the supplemental video.

When one looks closer at Table 3, though, it becomes apparent that this high rate of overall accuracy is very misleading. Almost 60 percent (6,893,753 pixels) of the total area sampled by the supplemental video was actually Cropland and Pasture. This class was among the easiest to classify as noted by its less than five percent omission errors and two percent commission errors. The misleadingly high overall accuracy resulted from this one severely over-sampled class.

Obviously, one must look at the accuracy of individual classes to get a correct sense of accuracy for the supplemental video classification. Of the seventeen observed classes in the supplemental video, only three classes, Cropland and Pasture, Black Hawthorn, and Open Water, had less than ten percent errors of commission and omission. Each of the remaining fourteen classes had at least ten percent errors of

Table 3: Supplemental Video-to-Field Classification Error Matrix

Supplemental Video \ Field	Douglas Fir	Douglas Fir / Red Alder / Bigleaf Maple	Douglas Fir / White Oak	Oregon Ash / Black Cottonwood / Bigleaf Maple	Oak Forest	Oak Woodland	Oregon White Oak / Douglas Fir - Bigleaf Maple	Shrub / Seed /Sapling	Black Hawthorn	Willow	Herbaceous Riparian	Cropland and Pasture	Orchards, Groves, Vineyards, Nurseries and Ornamental Horticultural Areas	Christmas Tree Plantations	Cottonwood Plantations	Residential	Open Water	TOTAL	ERRORS OF COMMISSION (proportion)
Douglas Fir	631,690	0	8,912	0	8,893	0	24,234	1	0	0	0	0	0	11,345	1,433	0	0	686,508	0.0799
Douglas Fir / Red Alder / Bigleaf Maple	43,017	86,468	0	0	0	0	0	0	0	0	0	0	0	0	0	0	0	129,485	0.3322
Douglas Fir / White Oak	153,846	4,102	382,842	9,882	4,765	0	47,203	0	0	0	0	792	6	2,548	0	0	0	605,986	0.3682
Oregon Ash / Black Cottonwood / Bigleaf Maple	0	0	2,379	454,754	10,217	0	9,272	0	0	11,296	1	3	0	0	0	0	0	487,922	0.0680
Oak Forest	53,506	0	43,249	6,133	217,205	0	27,517	0	0	0	0	2	0	0	0	0	0	347,612	0.3752
Oak Woodland	6,293	0	0	10,466	0	48,057	30,891	12,739	2,154	23,856	0	464	0	0	0	1,771	0	136,691	0.6484
Oregon White Oak / Douglas Fir - Bigleaf Maple	9,267	0	42,585	15,354	18,950	2,890	43,505	0	7,608	0	0	2	0	0	0	0	0	140,161	0.6896
Shrub / Seed / Sapling	0	0	1	0	0	3,501	2	877,178	1,835	0	0	29,766	7,646	125,645	0	0	0	1,045,572	0.1611
Black Hawthorn	0	0	0	6,511	0	0	0	0	328,814	0	2,136	0	0	0	0	0	0	335,261	0.0258
Willow	0	0	0	1,276	0	0	0	0	7,283	16,432	0	0	0	0	0	0	0	24,991	0.3425
Herbaceous Riparian	0	0	0	2,376	0	0	0	0	5,354	0	34,958	0	0	0	0	0	0	42,688	0.1811
Cropland and Pasture	5	0	4,620	633	3,072	0	23,024	11,103	1	1	0	6,551,594	14,471	61,861	0	0	0	6,670,385	0.0178
Orchards, Groves, Vineyards, Nurseries and Ornamental Horticultural Areas	0	0	0	0	0	0	0	0	0	0	0	0	67,472	0	0	0	0	67,472	0.0000
Christmas Tree Plantations	2,376	0	0	0	867	4,474	7,433	0	8,305	0	0	311,129	128,147	254,760	15,151	0	0	732,642	0.6523
Cottonwood Plantations	0	0	0	0	0	0	0	0	0	0	0	0	0	0	53,607	0	0	53,607	0.0000
Residential	0	0	0	0	0	0	0	0	0	0	0	1	0	0	0	10,602	0	10,603	0.0001
Open Water	0	0	0	0	0	0	0	0	0	0	0	0	0	0	0	0	94,155	94,155	0.0000
TOTAL	900,000	90,570	484,588	507,385	263,969	58,922	213,081	901,019	359,154	51,585	37,095	6,893,753	217,742	456,159	70,191	12,373	94,155	11,811,741	
ERRORS OF OMISSION (proportion)	0.2981	0.0453	0.2100	0.1037	0.1772	0.1844	0.7958	0.0906	0.0906	0.6815	0.0576	0.0496	0.6901	0.4415	0.2363	0.1431	0.0000		0.1257

OVERALL ACCURACY: 87.43%

omission and/or commission, and ten of these classes had more than 20 percent. Errors of omission were greatest for the following classes: 1) Oregon White Oak / Douglas Fir - Bigleaf Maple (80%); 2) Orchards, Groves, Vineyards, Nurseries and Ornamental Horticultural Areas (69%); 3) Willow (68%); 4) Christmas Tree Plantations (44%); 5) Douglas Fir (30%); 6) Cottonwood Plantations (24%); and 7) Douglas Fir / Oregon White Oak (21%). Errors of commission were highest in the following classes: 1) Oregon White Oak / Douglas Fir - Bigleaf Maple (69%); 2) Christmas Tree Plantations (65%); 3) Oak Woodland (65%); 4) Oak Forest (38%); 5) Douglas Fir / Oregon White Oak (37%); 6) Willow (34%); and 7) Douglas Fir / Red Alder / Bigleaf Maple (33%).

While some of the error encountered in the manual interpretation of the supplemental video can be attributed to "fuzziness" among classes as in the ODFW video interpretation, the majority of the error is due to low video quality. As stated previously, the supplemental video has a very hazy appearance (Figure 5) resulting from being recorded at a high altitude and the affects of atmospheric scattering. Color, tone and texture were, therefore, much less useful in the video interpretation, and much of the interpretation relied on shape, association and site. The reliance on these particular visual cues explains most of the successes and failures of the supplemental video interpretation. Classes with higher accuracy, such as Open Water, Cropland and Pasture, Black Hawthorn, and Oregon Ash / Black Cottonwood / Bigleaf Maple, are relatively easy to detect in the video by their shape and site. For example, cropland usually occurs in large areas with straight edges, and Oregon Ash / Black Cottonwood / Bigleaf Maple typically follows stream networks. In contrast, to successfully distinguish Douglas Fir from Douglas Fir / Oregon White Oak, the visual cues of color and texture become much more important. An additional factor contributing to the higher error of the supplemental video interpretation was the lack of large-scale zoomed video. The entire supplemental video interpretation was performed using only 1:2,400 scale video as compared to the 1:1,800 and 1:150 zoomed ODFW video.

Table 4: ODFW Video-to-Field Random Point Error Matrix

ODFW Video \ *Field*	Douglas Fir	Douglas Fir / Western Hemlock / Western Red Cedar	Douglas Fir / Red Alder / Bigleaf Maple	Red Alder / Bigleaf Maple	Shrub / Seed / Sapling	Cropland and Pasture	Christmas Tree Plantations	TOTAL	ERRORS OF COMMISSION (proportional)
Douglas Fir	73	1	1	0	0	0	0	75	0.0267
Douglas Fir / Western Hemlock / Western Red Cedar	0	0	0	0	0	0	0	0	0.0000
Douglas Fir / Red Alder / Bigleaf Maple	20	0	55	0	0	0	0	75	0.2667
Red Alder / Bigleaf Maple	0	0	0	75	0	0	0	75	0.0000
Shrub / Seed / Sapling	0	0	0	0	72	0	0	72	0.0000
Cropland and Pasture	0	0	0	0	0	75	0	75	0.0000
Christmas Tree Plantations	0	0	1	0	0	0	74	75	0.0133
TOTAL	93	1	55	75	72	75	74	447	
ERRORS OF OMISSION (proportional)	0.2151	1.0000	0.0351	0.0000	0.0000	0.0000	0.0000		*0.0515*

OVERALL ACCURACY: **94.85%**

Table 5: Supplemental Video-to-Field Random Point Error Matrix

Supplemental Video \ *Field*	Douglas Fir	Douglas Fir / Red Alder / Bigleaf Maple	Douglas Fir / White Oak	Oregon Ash / Black Cottonwood / Bigleaf Maple	Oak Forest	Oak Woodland	Oregon White Oak / Douglas Fir - Bigleaf Maple	Shrub / Seed /Sapling	Black Hawthorn	Willow	Cropland and Pasture	Orchards, Groves, Vineyards, Nurseries and Ornamental Horticultural Areas	Christmas Tree Plantations	Cottonwood Plantations	Residential	Open Water	TOTAL	ERRORS OF COMMISSION (proportion)
Douglas Fir	56	0	0	0	0	0	2	0	0	0	0	0	1	0	0	0	59	0.0508
Douglas Fir / Red Alder / Bigleaf Maple	20	47	0	0	0	0	0	0	0	0	0	0	0	0	0	0	67	0.2985
Douglas Fir / White Oak	23	1	41	2	0	0	8	0	0	0	0	0	0	0	0	0	75	0.4533
Oregon Ash / Black Cottonwood / Bigleaf Maple	0	0	1	71	1	0	1	0	0	1	0	0	0	0	0	0	75	0.0533
Oak Forest	11	0	5	1	53	0	5	0	0	0	0	0	0	0	0	0	75	0.2933
Oak Woodland	4	0	0	2	0	32	18	6	0	9	0	0	0	0	3	0	74	0.5676
Oregon White Oak / Douglas Fir - Bigleaf Maple	5	0	21	4	11	0	19	0	2	0	0	0	0	0	0	0	62	0.6935
Shrub / Seed / Sapling	0	0	0	0	0	0	0	56	0	0	1	0	11	0	0	0	68	0.1765
Black Hawthorn	0	0	0	1	0	0	0	0	74	0	0	0	0	0	0	0	75	0.0133
Willow	0	0	0	0	0	0	0	0	0	0	0	0	0	0	0	0	0	0.0000
Cropland and Pasture	0	0	0	0	0	0	1	1	0	0	71	0	2	0	0	0	75	0.0533
Orchards, Groves, Vineyards, Nurseries and Ornamental Horticultural Areas	0	0	0	0	0	0	0	0	0	0	0	75	0	0	0	0	75	0.0000
Christmas Tree Plantations	1	0	0	0	0	2	0	0	0	0	30	18	23	1	0	0	75	0.6933
Cottonwood Plantations	0	0	0	0	0	0	0	0	0	0	0	0	0	75	0	0	75	0.0000
Residential	0	0	0	0	0	0	0	0	0	0	0	0	0	0	0	0	0	0.0000
Open Water	0	0	0	0	0	0	0	0	0	0	0	0	0	0	0	75	75	0.0000
TOTAL	120	48	68	81	65	34	54	63	76	10	102	93	37	76	3	75	1,005	
ERRORS OF OMISSION (proportion)	0.5333	0.0208	0.3971	0.1235	0.1846	0.0588	0.6481	0.1111	0.0263	1.0000	0.3039	0.1935	0.3784	0.0132	1.0000	0.0000		0.2358

OVERALL ACCURACY: 76.42%

4.1.3 Additional Evaluation of Manual Video Interpretation

The error matrices in Tables 4 and 5 were developed in an attempt to obtain more meaningful overall accuracy statistics for the video interpretations by equalizing the number of samples for each class. Seventy-five random sample points (see Chapters 1 and 3) were generated for each class in the manually interpreted ODFW and supplemental video. Classes with less than 50 acres and/or less than 3 polygons were omitted from the matrices to help reduce the negative effects of the small sample area. It should be re-emphasized that the resulting accuracy statistics will still be contaminated by the negative effects of spatial autocorrelation as discussed in Chapters 1 and 3. Also, note that any class from the manually interpreted video having less than 75 samples in the error matrices resulted from the inaccessibility of sample points in the field. These points were omitted from the analysis.

Table 4 shows an overall accuracy of 94.85% for the six classes meeting the above criteria in the ODFW manual video interpretation. In comparison, the supplemental video matrix in Table 5 shows an overall accuracy of 76.42% for the 14 classes sampled. These statistics appear more realistic than those derived in the pixel-to-pixel matrices. The ODFW video interpretation, given the video's higher spectral quality and its addition of zoom-scale samples, was expected to be more accurate than the supplemental video.

4.1.4 Summary of Manual Video Interpretation

The evaluation of the manually interpreted video error matrices suggests that manual interpretations of airborne videography can be highly accurate if the video is acquired at a large scale, from a relatively low altitude, and if the classification scheme is not too complex. The overall accuracy of the ODFW video interpretation approached 95%. The main source of error in this video was between the Douglas Fir and Douglas

Fir / Red Alder / Bigleaf Maple classes. This error resulted primarily from "fuzziness" in the classification system and from the inexperience of the interpreter. The supplemental video interpretation proved to be significantly less accurate overall and when viewed class by class. Low spectral resolution, resulting from a high flying altitude combined with atmospheric scattering, and a lack of zoom-scale video caused most of this observed error. Additionally, there were more vegetation types to distinguish between in the area sampled by the supplemental videography than in the area sampled by the ODFW videography. The lack of sample independence was also responsible for some of the error in both video interpretations. Chapter 5 will address how these and other problems can be addressed in future studies.

4.2 Accuracy Assessment of ODFW Vegetation Map

The field verified video transects were used to determine the accuracy of the ODFW Landsat-based vegetation map for the Luckiamute / Rickreall study area. Tables 6 and 7 contain error matrices that evaluate the ODFW vegetation classification using an equalized random point sub-sample of the areas sampled by the video transects. The following sections explain and summarize these error matrices.

4.2.1 Evaluation of Error Matrices

The error matrix in Table 6 is based on 50 random sample points for each vegetation type classified by ODFW in their study area map. The Red Alder / Maple Forest and Red Alder / Conifer classes were evaluated separately since they were not present in the ODFW map but were found in the field. Table 6 shows an overall accuracy of the ODFW vegetation classification of slightly less than 62 percent. Since this accuracy level was significantly lower than anticipated, all recorded errors in Table 6 were checked to see if they were the result of georegistration mistakes.

Table 6: ODFW Vegetation Map-to-Field Verified Video Error Matrix

Field Verified Video / *ODFW Vegetation Map*	Douglas Fir Forest	Douglas Fir / White Oak	Red Alder Forest	Red Alder /Maple Forest	Red Alder / Conifer	Cottonwood Riparian Gallery	Oak Forest	Willow-Hawthorn	Shrub Dominant	Agriculture	Open Water	TOTAL	ERRORS OF COMMISSION (proportion)
Douglas Fir Forest	37	1	0	1	5	0	2	0	4	0	0	50	0.2600
Douglas Fir / White Oak	10	2	0	0	0	6	15	0	0	17	0	50	0.9600
Red Alder Forest	3	0	0	0	35	0	0	0	12	0	0	50	1.0000
Red Alder / Maple Forest	0	0	0	0	0	0	0	0	0	0	0	0	0.0000
Red Alder / Conifer	0	0	0	0	0	0	0	0	0	0	0	0	0.0000
Cottonwood Riparian Gallery	0	0	0	0	0	36	4	0	1	8	1	50	0.2800
Oak Forest	0	2	0	0	0	3	21	0	0	24	0	50	0.5800
Willow-Hawthorn	0	0	0	0	0	1	0	48	0	1	0	50	0.0400
Shrub Dominant	4	2	0	0	0	0	0	0	36	8	0	50	0.2800
Agriculture	0	0	0	1	0	0	0	0	0	49	0	50	0.0200
Open Water	0	0	0	0	0	0	0	0	0	2	48	50	0.0400
TOTAL	54	7	0	2	40	46	42	48	53	109	49	450	
ERRORS OF OMISSION (proportion)	**0.3148**	**0.7143**	**0.0000**	**1.0000**	**1.0000**	**0.2174**	**0.5000**	**0.0000**	**0.3208**	**0.5505**	**0.0204**		***0.3844***

OVERALL ACCURACY: **61.56%**

Table7: ODFW Map-to-Field Verified Video Error Matrix - Rectification Corrected

Field Verified Video / ODFW Vegetation Map	Douglas Fir Forest	Douglas Fir / White Oak	Red Alder Forest	Red Alder /Maple Forest	Red Alder / Conifer	Cottonwood Riparian Gallery	Oak Forest	Willow-Hawthorn	Shrub Dominant	Agriculture	Open Water	TOTAL	ERRORS OF COMMISSION (proportion)
Douglas Fir Forest	40	1	0	1	3	0	1	0	4	0	0	50	0.2000
Douglas Fir / White Oak	8	7	0	0	0	6	15	0	0	14	0	50	0.8600
Red Alder Forest	1	0	2	0	35	0	0	0	12	0	0	50	0.9600
Red Alder / Maple Forest	0	0	0	0	0	0	0	0	0	0	0	0	0.0000
Red Alder / Conifer	0	0	0	0	0	0	0	0	0	0	0	0	0.0000
Cottonwood Riparian Gallery	0	0	0	0	0	44	4	0	1	1	0	50	0.1200
Oak Forest	0	1	0	0	0	3	31	0	0	15	0	50	0.3800
Willow-Hawthorn	0	0	0	0	0	1	0	49	0	0	0	50	0.0200
Shrub Dominant	0	0	0	0	0	0	0	0	42	8	0	50	0.1600
Agriculture	0	0	0	0	0	0	0	0	0	50	0	50	0.0000
Open Water	0	0	0	0	0	0	0	0	0	0	50	50	0.0000
TOTAL	49	9	2	1	38	54	51	49	59	88	50	450	
ERRORS OF OMISSION (proportion)	**0.2041**	**0.2222**	**0.0000**	**1.0000**	**1.0000**	**0.1852**	**0.3922**	**0.0000**	**0.2881**	**0.4318**	**0.0000**		***0.3000***

OVERALL ACCURACY: **70.00%**

Twenty-two percent (38 out of 173) of the errors in Table 6 were found to be registration errors. These errors corresponded to the error found when georectifying the video transects to the Landsat imagery. All of the registration errors found near the centers of the video mosaics were less than 30 meters and most were less than 10 meters. Registration errors near the edges of the video mosaics were up to 90 meters. The error matrix in Table 7 incorporates these registration corrections into the accuracy assessment of the ODFW vegetation map.

The corrected error matrix in Table 7 shows an overall accuracy of 70 percent. While this accuracy level is still less than desired, most of the error is easily explainable when the vegetation classes are looked at individually.

Errors of omission and commission for the Douglas Fir Forest class were both approximately 80 percent. Errors of commission occurred mostly in the Red Alder / Conifer and Shrub Dominant classes. These few errors are likely the result of fuzzy classification error and time-delay, respectively. Determining the exact percentage of each tree species in an area is difficult both in the field and in satellite imagery interpretation. If the amount of conifer was near the 65% cutoff (greater than 65% Douglas fir is classified as Douglas Fir Forest and less than 65% Douglas fir with at least 33% red alder is Red Alder / Conifer), an error could have been made by either the field interpreter or the image classifier. It will be seen that much of the error revealed in this analysis falls into this fuzzy classification type. This type error could be reduced in future studies if a fuzzy sets approach can be successfully adopted. The Shrub Dominant class points that were incorrectly classified as Douglas Fir Forest are probably due to the approximate three year delay between the satellite image acquisition and the field verification. Active timber harvesting was observed in much of the western portion of the study area during the field verification portion of this study, and these forests were likely harvested between satellite acquisition and field classification. Therefore, the Douglas Fir Forest classification should not be considered incorrect. Douglas Fir Forest

omissions were most often mislabeled as Douglas Fir / White Oak. Again, these are probably most often fuzzy classification errors.

In addition to Douglas Fir Forest being mislabeled as Douglas Fir / White Oak, Oak Forest, Agriculture, and Cottonwood Riparian Gallery were often incorrectly classified as Douglas Fir / White Oak as well. These classification errors yielded an estimated 86 percent commission error for the Douglas Fir / White Oak class while omission errors were calculated at a reasonable 22 percent. Again, it is obvious that Oak Forest and Douglas Fir / White Oak disagreements probably resulted from fuzzy classification error. The surprisingly high amount of agriculture that was mislabeled as Douglas Fir / White Oak became less of a surprise when these points were looked at individually. All of these points were either Christmas tree plantations or orchards. Both of these classes typically have spectral signatures similar to the Douglas Fir / White Oak and the Oak Forest vegetation types. The confusion of Cottonwood Riparian Gallery and Douglas Fir / White Oak is also an error caused by similar spectral signatures. Additionally, Douglas Fir / White Oak often occurs in pockets next to riparian corridors which increases the difficulty of distinguishing these classes.

Cottonwood Riparian Gallery had an estimated 12 percent commission error and 18.5 percent omission error. The mislabeling of this class as Douglas Fir / White Oak was already discussed. As with that misclassification, the confusion of Oak Forest for Cottonwood Riparian and Cottonwood Riparian for Oak Forest was caused by the problem of differentiating similar spectral signatures.

In addition to the confusion with Cottonwood Riparian Gallery, Oak Forest was more significantly confused with Douglas Fir / White Oak and Agriculture. The relatively high estimated omission error rate of 39 percent was caused mostly by mislabeling Oak Forest as Douglas Fir / White Oak. As previously mentioned, this is primarily the result of fuzzy classification error. The high commission error rate of 38 percent for Oak Forest resulted from mislabeling the Agriculture class. As with the

Agriculture points mislabeled as Douglas Fir / White Oak, these fifteen points were all either Christmas tree plantations or orchards. Likewise, incorrect classification of these points was caused by problems differentiating the similar spectral signatures emitted by these vegetation types.

All of the red alder classes had very high, yet misleading, classification errors. The error matrix in Table 7 shows that Red Alder Forest had a 96 percent commission error. The confusion of Red Alder / Conifer as Red Alder Forest could be reasonably explained as fuzzy classification error and/or as resulting from the two vegetation types having similar spectral signatures. Additionally the misclassification of Shrub Dominant as Red Alder Forest could be satisfactorily explained as a time difference error. While these explanations are probably true, the extent of the misclassification is likely overstated due to an insufficient sample size and sampling scheme. For example, 31 of the 35 Red Alder Forest - Red Alder / Conifer mislabeled random points were in only three polygons. Likewise, eight out of the twelve Shrub Dominant points mislabeled as Red Alder Forest were in one polygon. Insufficient sample size can also explain some of the high error found in the Douglas Fir / White Oak - Oak Forest (13 out of 15 points in three polygons) and Oak Forest - Agriculture confusion (12/15 points in three polygons). Less error would be expected in these classes if more airborne videography had been available for the study area and if the video had been acquired to specifically sample the Luckiamute/Rickreall watersheds.

The Red Alder / Maple Forest and Red Alder / Conifer classes were not present in the ODFW map where the video transects sampled the study area but were in the field verified video classification. Therefore, these classes were analyzed by comparing their occurrences in the videography to the map. There were four polygons in the video classified as Red Alder / Maple Forest. Two of these were classified as Cottonwood Riparian Gallery and two as Douglas Fir Forest in the ODFW vegetation map. The confusion with Cottonwood Riparian Gallery is understandable since they can have

similar spectral signatures and the occurrences were in the transition zone of the valley floor to the Coast Range mountains. The occurrences of Red Alder / Maple Forest confused with Douglas Fir Forest are a result of the 30 meter spatial resolution of the Landsat TM imagery and the four hectare minimum mapping unit. Continuous four hectare areas of this vegetation could not be sensed by the satellite since Red Alder / Maple Forest typically occurs in long narrow corridors following stream networks. The field verified video contained eleven Red Alder / Conifer polygons. The ODFW map classified eight of these as Douglas Fir Forest and three as Red Alder / Douglas Fir Forest. Again, most of these errors are fuzzy classification errors.

The remaining classes in the Table 7 error matrix had relatively high estimated levels of accuracy. Willow-Hawthorn had a surprisingly low commission error of two percent and omission error of zero percent. Shrub Dominant had an estimated sixteen percent commission error and 29 percent omission error. The omission errors have already been explained as time difference errors as opposed to misclassification errors. The confusion of Agriculture with Shrub Dominant results from a combination of fuzzy classification error and similar spectral signatures. Abandoned pastures caused the confusion. The distinction between these classes was often difficult to make during the field verification. Agriculture had an estimated commission error of zero percent. The high omission error of 76 percent has previously been explained as either fuzzy classification error or as orchards and Christmas tree plantations having similar spectral signatures as several natural vegetation types. Open Water, as anticipated, had zero percent commission and omission errors.

4.2.2 Summary of ODFW Map Accuracy Assessment

The overall accuracy of the ODFW Luckiamute / Rickreall vegetation map was estimated at 70 percent after compensating for georegistration errors. The classes that met or exceeded the 80 percent accuracy goal were Douglas Fir Forest, Cottonwood

Riparian Gallery, Willow-Hawthorn, and Shrub Dominant. There were no commission errors for the Agriculture class, but omission errors were estimated at 76 percent. This confusion resulted from mistaking orchards and Christmas tree plantations for Douglas Fir / White Oak or Oak Forests and abandoned pasture for Shrub Dominant. The remaining vegetation classes were estimated at less than 80 percent accuracy. In addition to the confusion of different vegetation types having similar spectral signatures, misclassifications were caused by fuzzy classification error, time delay of accuracy assessment, limitations in spatial resolution of Landsat TM data, and/or by an inadequate sampling scheme and size.

The small sample size and less-than-desirable sampling scheme limit the confidence of these error estimates. However, it is obvious that Christmas tree plantations and orchards are being confused with Douglas Fir / White Oak and Oak Forest too often as are Red Alder Forest with Red Alder / Conifer and Douglas Fir / White Oak with Oak Forest. Additional effort and interpretation techniques will be necessary for ODFW to better distinguish these vegetation types of similar spectral signatures. Additionally, successfully adopting a fuzzy-sets approach in any future accuracy assessment will result in a more accurate estimation of error for these classes.

5. CONCLUSIONS

The major goal of this research was to determine how and to what extent airborne videography can replace field verification in the assessment of classification-accuracy for satellite-based vegetation maps. To fulfill this goal, an accuracy assessment strategy, incorporating airborne videography and a Landsat TM-based vegetation map created by ODFW, was developed and tested on a pilot study area consisting of the Luckiamute and Rickreall watersheds. The following section summarizes the findings of these efforts. These results are then applied to outline how ODFW might assess the remainder of their Oregon GAP vegetation map. Finally, recommendations are presented for using airborne videography in future Landsat TM-based vegetation map classification and validation efforts.

5.1 Evaluation of Airborne Videography

The results of this research indicate that airborne videography has limited usefulness as a tool for Landsat TM-based vegetation map validation. Despite the facts that collecting it can be substantially faster than field work and that it allows remote, inaccessible-by-ground areas to be sampled, using airborne videography is not an efficient method for assessing the accuracy of most satellite derived vegetation maps. First, the cost of acquiring airborne videography, while cheaper than traditional aerial photography, is still quite expensive. For example, the ODFW video acquired in this study cost $30,000 in 1993. As will be discussed in the next section, a more costly, increased-density of flight-lines in a more complex sampling scheme would be necessary to sufficiently assess the accuracy of the ODFW state vegetation map. Second, the accuracy of the video interpretation must be assessed before it can be used to assess the accuracy of the satellite based map. Therefore, a certain amount of field work must still

be performed when using airborne videography. The collection of enough field points to perform this assessment will likely be difficult as it depends on having a sufficient number of video sample points for each vegetation class within observation distance of an accessible road. Additionally, this substitution of interpreted videography for "ground-truth" data will yield a more complex, if not questionable, statistical analysis in the final assessment. Finally, the inferior spectral resolution of airborne video makes successful interpretation of vegetation classes difficult. In this study, a misleading overall interpretation accuracy of nearly 95 percent was obtained for the higher resolution ODFW video. However, this video was recorded in a relatively small area of low vegetation diversity, and interpretation accuracy was substantially lower for mixed species classes in this video as well as in the supplemental video. These findings indicate that airborne videography will be less suitable for accuracy assessment as the vegetation classification and landscapes increase in complexity (southwestern Oregon for example).

Despite its limited value as an accuracy assessment tool, airborne videography would be a valuable classification aid in the development of a satellite based vegetation map. GPS georeferenced airborne video could be used to quickly generate training areas for supervised classifications or to help label classes resulting from unsupervised classifications of satellite imagery. Proper planning of video acquisition is the key to its successful use for these purposes. The final section of this chapter will address this topic.

5.2 ODFW Accuracy Assessment of Oregon Vegetation Map

5.2.1 Using Airborne Videography

Based on the results of this research, it is recommended that the airborne videography acquired by ODFW not be used for the accuracy assessment of the ODFW

Oregon vegetation map. There are several reasons for this recommendation. First, many of the vegetation classes included in the state map will be under-sampled. For example, there are three video flight lines that partially intersect the Willamette Valley. None of these lines capture the transition zone between the valley floor and the Coast Range mountains. Therefore, classes, such as Red Alder / Cottonwood Riparian Gallery, that occur mostly in this zone will be under-sampled. A stratified systematic random sample, dividing the state into physiographic regions (Figure 15) with transects planned to capture the greatest vegetation diversity within these regions, would have produced a more inclusive sample, however, at a significantly higher cost. For example, if the transects in the Willamette Valley were flown east-to-west, the transition zones within the valley would have been better captured. Second, if videography is used, field work throughout the state will still be required to assess the video interpretation before it can be used in the accuracy assessment. Additionally, the calculated error within the interpreted video samples will have to be statistically incorporated into the final accuracy assessment of the vegetation map. The resulting method would likely be statistically less valid or would at least reduce the confidence of the accuracy assessment for some classes. Moreover, the accuracy assessment of the vegetation map could never be higher than the per-class assessment accuracy from the video samples. Third, there would be some inaccuracy from using the videography to assess a 100 hectare minimum mapping unit map. A frame of the ODFW pan-scale video is approximately 1000 meters wide and contains only 70 hectares in area. While the video zooms may allow an accurate interpretation at a point, the pan-scale video are not at a small enough scale to consistently extract how a point will fit into the 100 hectare MMU classification. If a sample point falls within a 100 hectare MMU vegetation polygon that is shaped long and narrow with the length parallel to the flight line, there will be more chance of accurately classifying that point. Finally, it is suspected that the interpretation of video in areas where several grasses or shrubs could potentially occur would be substantially less

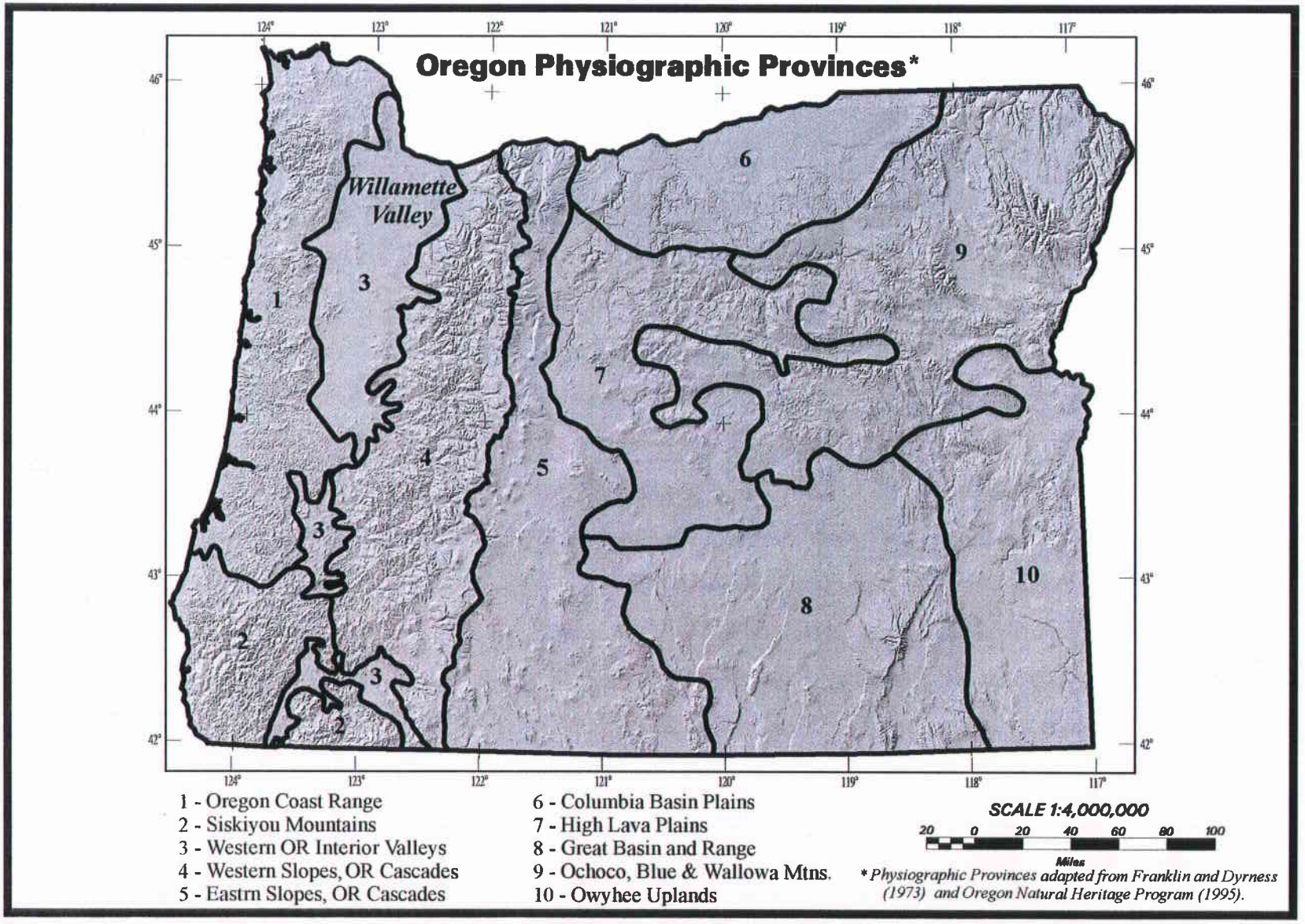

Figure 15: Map of Physiographic Provinces of Oregon

accurate than the accuracy recorded in this pilot study. The spatial and spectral resolution of the video is probably too poor to differentiate these types of classes. There were no such similar classes in the sample study area to test this theory, but viewing video samples from other portions of the state indicate that interpretation of these areas would be difficult.

Should ODFW decide to use the existing airborne videography despite these shortcomings, the following general methodology should be adopted. A point sample should be generated from the ODFW videography by interpreting the video, displayed on a television, every time the video zooms. When interpreting the video, not only should the zoomed point be considered, but the surrounding area in the pan-scale video should be also. In other words, it should be remembered that the map to be assessed has merged all vegetation polygons smaller than 100 hectares. The interpretations should be recorded in a digital database along with the GPS time indicated on the zoomed point video frame. Once a video flight line has been interpreted, the resulting database can be geocoded by linking it, via the GPS time, to the corresponding GPS ARC/INFO point coverage. Since the GPS coverages only have ground locations recorded once every second and the video is recorded at 30 frames per second, it may be desirable to interpolate the ground location. This is easily accomplished using the interpreted video frame number (0-30) and the locations of the two recorded GPS seconds that the frame falls between. This entire geocoding process can be easily automated by converting the interpreted database to an ARC/INFO table and writing an ARC/INFO AML (Arc Macro Language). The AML should output a new point coverage containing the interpreted video sample points.

Once all the video flight lines are interpreted, the resulting sample point coverages may be appended together into one coverage for the final analysis. Alternatively, since the state map was developed by physiographic regions, the point coverage may be split up and assessed by these regions if desired. Either way, the point coverage will then need to be exported to image processing software to produce an accuracy assessment of the state

coverage will then need to be exported to image processing software to produce an accuracy assessment of the state vegetation coverage using these video sample points (or an equal interval sub-sample of these points) as the ground control points.

As previously stated, an estimate of the accuracy of the video interpretation would have to be incorporated into the final vegetation map accuracy analysis. The assessment of the video interpretation accuracy can be facilitated by using ARC/INFO to determine which of the video sample points fall within a potentially viewable distance of a road (e.g., 500 meters or less). These points may then be field verified and subsequently assessed in a similar manner as described above.

5.2.2 Recommended Accuracy Assessment Methodology

Again, because of the shortcomings and problems described already, the results of this research do not endorse using this airborne videography methodology to assess the state vegetation map. Instead of using videography supplemented with field verification, a method using field verification only will yield a more accurate classification assessment without greatly increasing the cost of field verification. Additionally, this field verification method will result in more classes being more completely sampled than would the videography method.

The field verification accuracy assessment process endorsed for the ODFW state vegetation map makes extensive use of GIS and GPS technologies. This methodology is currently being developed and tested on a large-scale vegetation mapping project of the Willamette Valley by members, including this researcher, of the ODFW Ecological Analysis Center. This process involves three major steps: 1)Generating field accessible random points; 2)Field verification; and 3)Analysis. The following paragraphs detail the procedures.

The first step of the process is to generate random points that have a high likelihood of being field accessible for each class in the vegetation map. First, buffers

are generated with ARC/INFO software around all of the roads in Oregon using an appended roads coverage of the 1:100,000 digital Census TIGER (Topologically Integrated Geographic Encoding and Referencing) files (available from the Oregon State GIS Service Center). These buffers would represent the reasonable average distance that one could expect to view sample points from the road when in the field. The Willamette Valley study has successfully used a distance of 500 meters on each side of a road. The optimal buffer, however, is yet to be determined and will probably vary depending on terrain and land cover. Second, the classified vegetation map is clipped, using ARC/INFO or Imagine software, by the road buffers so that only the classified areas within the road buffers remain. Third, random points are generated with Imagine for each vegetation class contained within the road buffers. Imagine provides an equal interval option when generating random points which ensures that all classes within the buffers are sufficiently sampled. If some classes have a very low proportion of the total area and/or relatively few polygons, the individual polygons for these classes can be field verified separately. As discussed in Chapter 2, between 50 and 100 random points should be generated for each class depending on the size of the area being assessed and the number of classes (Congalton, 1996). For the statewide map, 100 random points should be generated for each class with the expectation of having at least 75 points that are field accessible for each class. That is because some of the points will be inaccessible due to closed or private roads, or visual obstructions such as trees. The Willamette Valley study, however, has found such impediments to be minimal.

The second major step of the process is field verification of the random points generated in the first step. This step integrates a laptop computer, Pen Metrics' Field Notes software, and a GPS receiver to digitally collect the field classification of each random point. First, the random points, roads coverage, and classified image need to be converted to a dBase DBF, AutoCAD DXF, and Geo-TIFF formats, respectively. All conversions can be performed with a combination of ARC/INFO, Imagine and Field

Notes software. Increased performance of Field Notes software usually results from partitioning the classified image into several smaller images for individual display. To enhance field location reference, one may also desire to create corresponding Geo-TIFF files of the raw satellite composites used to create the vegetation classification. Next, all of these data are transferred to a vehicle-mounted laptop computer with Field Notes software and an attached GPS unit with externally mounted antennae. Then, with the TIFF images, roads file, random points, and real-time GPS location being displayed simultaneously, at any desired magnification on the Field Notes computer screen, one can easily locate and verify the random points.

The final major step of this accuracy assessment process is the analysis. The field collected data may be converted back into Imagine for the analysis. However, unless one wants to assess the spatial distribution of the inaccuracies in detail, it is probably easier to use a statistical analysis software package or spreadsheet software such as Microsoft Excel. Standard error matrices as well as advanced statistics can be developed with these programs. Additionally, as the results in Chapter 4 explained, the use of fuzzy-sets would make the assessment even more meaningful. Using the Field Notes as just described would allow additional data such as classification confidence to be collected digitally, real-time in the field for such an analysis.

While the field-based assessment procedure described here is not ideal, it appears to have more advantages than airborne videography-based methods. Although all of the roads delineated in the 1:100,000 TIGER files may not be accessible due to access and private land issues, using these as a sample base should still provide good coverage of Oregon. The two main drawbacks of the field-based technique are that it is slow and rather expensive. Based on the ODFW Willamette Valley study, it would probably take one person approximately 12 months to sample the entire state. However, the cost of this would probably be similar to or cheaper than recording airborne videography for the state if the sampling scheme were stratified by physiographic region as suggested previously.

Furthermore, there would be the additional cost to the videography-based method for field verifying the video interpretation. Overall, the field-based method will produce significantly better results at a cost similar to or less than the airborne videography method with the disadvantage of taking more person-hours to complete.

5.3 Future Map Classification and Validation with Airborne Videography

This research has shown that airborne videography is better suited for satellite-based vegetation map classification than for validation. For either use, the videography sampling should be stratified by physiographic region to promote a more representative sample of the vegetation classes. Within these strata, a systematic random grid of flightlines, such as the scheme used by Slaymaker et al. (1996), would be preferable to systematic transects in only one orientation. While costlier to acquire, this sampling scheme will promote a more representative sampling of the landscape's actual vegetation.

The usefulness of airborne videography as a validation technique is primarily limited by the persisting need to perform field verification. This research revealed that the visual interpretation of airborne videography will not be perfect. The greater the landscape complexity being mapped and the more diverse the vegetation classification, the less accurate will be the interpretation. Statistical validation of such a video interpretation and any accuracy assessment based on it will mandate a field verification throughout the mapped area. Therefore, a "field verification only" accuracy assessment method will usually be more efficient than incorporating airborne videography. Other problems limiting the usefulness of airborne videography in accuracy assessment include ensuring a representative sample of all vegetation classes, and recording the videography at scales that accommodate successful interpretation with respect to the satellite-based map's minimum mapping unit.

Airborne videography may have more promise as a satellite-based vegetation map classification aid. Using a stratified systematic random sampling technique as previously

outlined, a large amount of point sample data, can be generated relatively quickly for use in developing training areas or labeling polygons resulting from unsupervised classifications. Since acquiring airborne videography is still somewhat expensive and its interpretation will not usually be totally accurate, using it to help classify areas for which there is no preexisting ground-collected data may be its most beneficial use.

Technological advancements may increase the usefulness of airborne videography as classification and validation aids in the near future. Digital video cameras complying to high definition television (HDTV) standards are already being developed (Airola, 1996). These cameras will greatly increase the potential spatial resolution of airborne videography which should yield increased visual interpretation accuracy. An attractive alternative to videography will likely be digital aerial photography. High-resolution digital cameras capable of capturing images in excess of 4 million pixels already exist (Airola, 1996). Airborne imagery captured by these cameras should also yield more accurate interpretations. Additionally, linking high-resolution digital cameras to a GPS and computer will allow point sample interpretations to be generated more quickly and spatially accurately than when using video cameras. The cameras could be activated at the exact time the GPS locations are received from the satellites, and subsequent visual interpretations could be added to the same digital database containing the GPS data. Despite these technological advancements, until the accuracy of visual interpretations resulting from imagery yielded by these cameras meets or exceeds field verification accuracy, the usefulness of these remote sensing technologies will be limited as validation aids for satellite-based maps.

BIBLIOGRAPHY

Airola, T. M. 1996. Emerging Technologies: Digital Aerial Photography -- An Overview. In: *Gap Analysis: A Landscape Approach to Biodiversity Planning.* Scott, J. M., T. H. Tear, and F. W. Davis (eds.). American Society for Photogrammetry and Remote Sensing. P.269-277.

Avery, T. E., and G. L. Berlin. 1992. *Fundamentals of Remote Sensing and Airphoto Interpretation.* 5th ed. Macmillan Publishing Company, New York.

Bishop, Y., S. Fienberg, and P. Holland. 1975. *Discrete multivariate analysis - theory and practice.* MIT Press, Cambridge, Ma. 575pp.

Bobbe, T., D. Reed, and J. Schramek. 1993. Georeferenced airborne video imagery. *Journal of Forestry.* August 1993:34-37.

Campbell, J. 1981. Spatial autocorrelation effects upon the accuracy of supervised classification of land cover. *Photogrammetric Engineering and Remote Sensing* 47:355-363.

Campbell, J. 1987. *Introduction to Remote Sensing.* Guilford Press, New York, NY. 551pp.

Chrisman, N. 1989. Modeling error in overlaid categorical maps. Pages 21-34 in Goodchild, M. and S. Gopal, editors. *Accuracy of spatial databases.* Taylor and Francis, Bristol, PA.

Cliff, A. D. and J. K. Ord. 1973. *Spatial Autocorrelation.* Pion Limited, London. 178pp.

Cohen, J. 1960. A coefficient of agreement for nominal scales. *Educational and Psychological Measurement.* 20:37-46.

Congalton, R. G. 1988a. Using spatial autocorrelation analysis to explore errors in maps generated from remotely sensed data. *Photogrammetric Engineering and Remote Sensing* 54:587-592.

Congalton, R. G. 1988b. A comparison of sampling schemes used in generating error matrices for assessing the accuracy of maps generated from remotely sensed data. *Photogrammetric. Engineering & Remote Sensing.* 54: 593-600.

Congalton, R. G. 1991. A review of assessing the accuracy of classifications of remotely sensed data. *Remote Sensing of the Environment.* 37: 35-46.

Congalton, R. G. 1996. Accuracy Assessment: A Critical Component of Land Cover Mapping. In: Gap Analysis: A Landscape Approach to Biodiversity Planning. Scott, J. Michael, Timothy H. Tear, and Frank W. Davis (eds.). American Society for Photogrammetry and Remote Sensing. P.119-131.

Congalton, R., and K. Green. 1993. A practical look at the sources of confusion in error matrix generation. *Photogrammetric. Engineering & Remote Sensing* 59:641-644.

Congalton, R. G., R. G. Oderwald, and R. A. Mead. 1983. Assessing Landsat classification accuracy using discrete multivariate statistical techniques. *Photogrammetric. Engineering & Remote Sensing.* 49:1671-1678.

Doyle, T. W., K. W. Krauss, C. J. Wells, and M. R. Roberts. 1994. The use of videography to assess the spatial impact of hurricanes on forest ecosystems. *GIS/LIS*, pp. 223-228. http://www.sgi.ursus.maine.edu/gisweb/spatdb/gis-lis/gi94028.html.

Eastman, J. R. 1992. *Idrisi Version 4.0 Technical Reference.* Clark University, Worcester, Massachusetts.

Edwards, G. J. 1982. Near-infrared aerial video evaluation for freeze damage. *Proc. Fla. State Hortical. Soc.*, 95:1-3.

Edwards, G. J., and P. M. Schumacher. 1989. Evaluating the spectral response of your video camera. *Proceedings 12th Biennial Workshop on Color Aerial Photography and Videography in the Plant Sciences.* American Society of Photogrammetry and Remote Sensing, Falls Church, VA. pp. 212-215.

Ehlers, M., R. J. Hintz, and R. H. Green. 1989. High resoultion airborne video system for mapping and GIS applications. *Proceedings 12th Biennial Workshop on Color Aerial Photography and Videography in the Plant Sciences.* American Society of Photogrammetry and Remote Sensing, Falls Church, VA. pp. 171-177.

Escobar, D. E. , R. L. Bowen, H. W. Gausman, and G. R. Cooper. 1983. Use of a near-infrared video recording system for the detection of freeze-damaged citrus leaves. *J. Rio Grande Valley Hortical. Soc.*, 36:61-66.

Everitt, J. H., D. E. Escobar, and R. Villareal. 1988. Evaluation of single-band-video and video-band-based indices for grassland phytomass assessment. *Photogrammetric Engineering & Remote Sensing* 54:1177-1180.

Everitt, J. H., D. E. Escobar, R. Villarreal, J. R. Noriega, and M. R. Davis. 1991 Airborne video systems for agricultural assessment. *Remote Sensing of the Environment*, 35:231-242.

Everitt, J. H., and P. R. Nixon. 1985. Video Imagery: A new remote sensing tool for range management. Journal of Range Management. 38(5):421-424.

Fitzpatrick-Lins, K. 1981. Comparison of sampling procedures and data analysis for a land-use and land-cover map. *Photogrammetric Engineering & Remote Sensing* 47:343-351.

Franklin, J. F., and C. T. Dyrness. 1973. Natural vegetation of Oregon and Washington. USDA Forest Service, General Technical Report PNW-8. Pacific Northwest Forest and Range Expiriment Station, Portland, Oregon. Reprinted Oregon State University Press, 1988.

Gerbermann, A. H., D. E. Escobar, and C. L. Wiegand. 1989. Comparison of aerial video, ground video and ground spectrometer data of field soils by wavelength and mapping unit. *Proceedings 12th Biennial Workshop on Color Aerial Photography and Videography in the Plant Sciences.* American Society of Photogrammetry and Remote Sensing, Falls Church, VA. pp. 178-186.

Ginevan, M. E. 1979. Testing land-use map accuracy: another look. *Photogrammetric Engineering and Remote Sensing* 47:1371-1377.

Goodchild, M. 1989. Modeling error in objects and fields. Pages 107-113 in Goodchild, M. and S. Gopal, editors. *Accuracy of spatial databases.* Taylor and Francis, Bristol, PA.

Gopal, S., and C. E. Woodcock. 1994. Theory and Methods for Accuracy Assessment of Thematic Maps Using Fuzzy Sets. *Photogrammetric. Engineering & Remote Sensing.* 60(2): 181-188.

Graham, L. A. 1993. Airborne video for near-real-time vegetation mapping. *Journal of Forestry.* 91(August):28-32.

Hudson, W. D., and C. W. Ramm. 1987. Correct formulation of the Kappa coefficient of agreement. *Photogrammetric. Engineering & Remote Sensing.* 53:421-422.

Hay, A. M. 1979. Sampling designs to test land-use map accuracy. *Photogrammetric. Engineering & Remote Sensing* 45:529-533.

Hord, R. M., and W. Brooner. 1976. Land use map accuracy criteria. *Photogrammetric. Engineering & Remote Sensing* 42:671-677.

Jennings, C. A., P. A. Vohs, and M. R. Dewey. 1992. Classification of a wetland area along the upper Mississippi River with aerial videography. *Wetlands.* 12(3):163-170.

Jensen, J. R. 1986. *Introductory Digital Image Processing: A remote sensing perspective.* Prentice-Hall, Englewood Cliffs, New Jersey.

Kagan, J., and S. Caicco. 1992. *Manual of Oregon actual vegetation.* Oregon Natural Heritage Program and Idaho Cooperative Fish and Wildlife Research Unit. Draft. 186pp.

King, D. J. 1991. Determination and reduction of cover type brightness variations with view angle in airborne multispectral video imagery. *Photogrammetric Engineering & Remote Sensing* 57:1571-1578.

King, D. J. 1992. Evaluation of radiometric quality, spatial resolution and statistical characteristics of multispectral videography. *Journal of Imaging Science and Technology* 36(4):394-404.

King, D. J., and J. Vlcek. 1990. Development of a multispectral video system and its application in forestry. *Canadian Journal of Remote Sensing* 16(1):15-22.

Lillesand, T., and R. Kiefer. 1994. *Remote Sensing and Image Interpretation.* 3rd ed. John Wiley and Sons, New York, NY. 750 pp.

Limaye, U. S., A. B. Bishop, C. M. U. Neale. 1994. Developing a Urban Land Cover GIS Layer using Multispectral Airborne Videography. *Http://www.declab. usu.edu: 8080/~sl5ns/paper1/p1-final.html.*

Lusch, D. P. 1988. Super-VHS for improved airborne CIR videography. *Proceedings First Workshop on Videography*, American Society of Photogrammetry and Remote Sensing, Falls Church, Virginia, pp. 23-29.

Ma, Z. and R. L. Redmond. 1995. Tau coefficients for accuracy assessment of classification of remote sensing data. 1995. *Photogrammetric Engineering & Remote Sensing.* 61(4):435-439.

Manzer, F. E., and G. R. Cooper. 1982. Use of portable video-taping for aerial infrared detection of potato disease. *Plant Disease*, 66:665-667.

Mausel, P. W., J. H. Everitt, D. E. Escobar And D. J. King. 1992. Airborne videography: current status and future perspectives. *Photogramm. Eng. & Remote Sensing* 58(8):1189-1195.

Mausel, P. W., G. Kalaluka, D. Mudderman, D. Escobar, and M. Davis. 1990. Multispectral video analysis of micro-relief dominated poorly drained soils in western Indiana. *Journal of Imaging Technology* 16:113-119.

Meisner, D. E. 1986. Fundamentals of Airborne Video Remote Sensing. *Remote Sensing of Environment* 19:63-79.

Milliken, Jeff A. And Curtis E. Woodcock. 1996. Integration of Inventory and Field Data for Automated Fuzzy Accuracy Assessment of Large Scale Remote-Sensing Derived Vegetation Maps in Region 5 National Forests. In: Spatial Accuracy Assessment in Natural Resources and Environmental Sciences: Second International Symposium May 21-23, 1996, Fort Collins, Colorado. P. 541-544.

O'Neil, T. A., R. J. Steidl, W. D. Edge, and B. Csuti. 1995. Using wildlife communities to improve vegetation classification for conserving biodiversity. *Conservation Biology* 9(6):1482-1491.

Oregon Natural Heritage Program. 1995. Rare, threatened and endangered plants and animals of Oregon. Oregon Natural Heritage Program, Portland, Oregon.

Palmer, R.A., R.C. Maggio, and P. T. Sprinz. 1987. Digital analysis of color infrared aerial video imagery. *Proceedings 11th Biennial Workshop on Color Aerial Photography and Videography in the Plant Sciences.* American Society of Photogrammetry and Remote Sensing, Falls Church, VA. pp. 280-285.

Rhode, W. G. 1978. Digital image analysis techniques for natural resources inventory. Pages 43-106 in *National Computer Conference Proceedings.*

Richards, J. A. 1993. *Remote Sensing Digital Image Analysis: An Introduction.* 2nd ed. Springer-Verlag, New York.

Richardson, A.J., J. H. Everitt, and D. E. Escobar. 1992. Calibration of gain compensated aerial video remote sensing imagery using ground reflections standard. *Proceedings 13th Biennial Workshop on Color Aerial Photography and Videography in the Plant Sciences.* American Society of Photogrammetry and Remote Sensing, Falls Church, VA.

Rosenfield, G. H. And K. Fitzpatrick-Lins. 1986. A coefficient of agreement as a measure of thematic classification accuracy. *Photogrammetric Engineering & Remote Sensing.* 52:223-227.

Rosenfield, G. H., K. Fitzpatrick-Lins, and H. Ling. 1982. Sampling for thematic map accuracy testing. *Photogrammetric Engineering & Remote Sensing* 48:131-137.

Russ, J. C. 1995. *The Image Processing Handbook,* 2nd ed. Boca Raton, FL: CRC Press.

Sayn-Wittgenstein, L. 1978. *Recognition of tree species on aerial photographs.* Information Report FMR-X-118. Forest Management Institute, Ottawa, Ontario.

Schlagel, J. 1995. Integrating aerial-videography with Arc/Info for satellite image interpretation and accuracy assessment in Vermont. *Fifteenth Annual ESRI User Conference Proceedings*. Palm Springs, CA.

Scott, J. M., F. Davis, B. Csuti, R. Noss, B. Butterfield, C. Groves, H. Anderson, S. Caicco, F. D'Erchia, T. C. Edwards, Jr., J. Ullman, and R. G. Wright. 1993. Gap Analysis: a geographic approach to protection of biological diversity. *Wildlife Monographs* 123:1-41.

Slaymaker, D. M., K. M. L. Jones, C. R. Griffin, and J. T. Finn. 1996. Mapping Deciduous Forests in Southern New England Using Aerial Videography and Hyperclustered Multi-Temporal Landsat TM Imagery. In: *Gap Analysis: A Landscape Approach to Biodiversity Planning*. Scott, J. M., T. H. Tear, and F. W. Davis (eds.). American Society for Photogrammetry and Remote Sensing. P.87-101.

Snider, M. A., J. W. Hayse, and I. Hlohowskyj. 1994. Multispectral airborne videography evaluates environmental impact. *GIS World*. June 1994, pp. 50-52.

Stehman, S. V. 1992. Comparison of systematic and random sampling for estimating the accuracy of maps generated from remotely sensed data. *Photogrammetric Engineering & Remote Sensing*. 58:1343-1350.

Stehman, S. V. 1996. Cost-effective, Practical Sampling Strategies for Accuracy Assessment of Large-Area Thematic Maps. In: Spatial Accuracy Assessment in Natural Resources and Environmental Sciences: Second International Symposium May 21-23, 1996, Fort Collins, Colorado. P.485-492.

Story, M., and Congalton, R. 1986. Accuracy assessment: a user's perspective. *Photogrammetric Engineering & Remote Sensing* 52:397-399.

Thomasson, J. A., C. W. Bennett, B. D. Jackson, and M. P. Mailander. 1994. Differentiating bottomland tree species with multispectral videography. *Photogrammetric Engineering & Remote Sensing*. 60(1):55-59.

Thorpe, J. 1993. Aerial photogrammetry: State of the industry in the US. *Photogrammetric Engineering & Remote Sensing* 59(11):1599-1604.

Tortura, R. 1978. A note on sample size estimation for multinomial populations. *The American Statistician* 32:100-102.

Van Genderen, J. L., and B. F. Lock. 1977. Testing land use map accuracy. *Photogrammetric Engineering and Remote Sensing* 43:1135-1137.

Vlcek, J. 1983. Videography: some remote sensing applications. *Proc. 49th Annual Meeting Am. Soc. Photogrammetry*, pp. 63-69.

Wanless, B. 1992. GPS/Positioned Digital Video for Airborne GIS Data Acquisition. *Journal of Surveying Engineering* 118(3):80-89.

Woodcock, Curtis E. 1996. On Roles and Goals for Map Accuracy Assessment: A Remote Sensing Perspective. In: Spatial Accuracy Assessment in Natural Resources and Environmental Sciences: Second International Symposium. May 21-23, 1996, Fort Collins, Colorado. P. 535-540.

Yuan, X. P., D. J. King, and J. Vlcek. 1991. Assessment of sugar maple decline based on spectral and textural analysis of multispectral aerial videography. *Remote Sensing of Environment* 37(1):47-54.